Collocated and non-collocated active spatial absorbers for spatial flexible structures

Petr Beneš[a], Jan Gregor[a], Wim Michiels[b], Tomáš Vyhlídal[c], Zbyněk Šika[a]

[a]*Department of Mechanics, Biomechanics and Mechatronics, Faculty of Mechanical Engineering, Czech Technical University in Prague, Technická 1902/4, 160 00 Praha 6, Czech Republic,*
Petr.Benes@fs.cvut.cz, Zbynek.Sika@fs.cvut.cz
[b]*Department of Computer Science, KU Leuven, Celestijnenlaan 200A, Leuven 3001, Belgium,*
Wim.Michiels@kuleuven.be
[c]*Department of Instrumentation and Control Engineering, Faculty of Mechanical Engineering, Czech Technical University in Prague, Technická 1902/4, 160 00 Praha 6, Czech Republic,*
Tomas.Vyhlidal@fs.cvut.cz

Abstract

This paper deals with the analysis and design of an active spatial mechanical vibration absorber and verification of its performance in collocated and non-collocated vibration absorption of a spatial flexible primary structure. The considered active absorber with six degrees of freedom has six identical natural frequencies. It is a so-called unifrequency absorber. The unifrequency property is achieved by delayed feedback, according to the concept of a delayed resonator. A proper tuning of the delayed feedback compensates the damping and variations in stiffness of mechanical parts, resulting in the behaviour of an ideal absorber. The absorber was attached to a three-dimensional flexible frame with many degrees of freedom transformed to a reduced order model in modal coordinates. The use of a unifrequency absorber for two types of tasks is shown in this paper. In the collocated case, the absorber is placed at the location where we want to suppress vibration. Such a placement is often not possible for various reasons. Therefore, the non-collocated absorber is also investigated that is remote from the point of desired vibration suppression. The absorber has considerable potential for use in improving the dynamic behaviour of robots, complex rotor systems and other mechanical systems suffering from unwanted fully spatial vibrations.

Keywords: Active vibration absorber; collocated absorber; non-collocated absorber; spatial unifrequency absorber, delayed resonator, spatial flexible primary structure;

1. Introduction

Vibrations play a negative role in many engineering applications. We can mention precision machining, surface finishing, precision instruments, surgical robots, precision industrial robots, etc. Therefore, much attention is paid to the development of vibration suppression methods. These involve a variety of approaches, e.g. input shaping [1], active vibration suppression using optimal control [2], or a combination of both feedforward and feedback control [3]. Adaptive active vibration suppression approaches allow the control system to adapt to the actual properties of the primary structure [4], [5]. A

different approach is vibration isolation using energy dissipation into damping elements [6]. Another common method, which is also used in this paper, is the use of a vibration absorber, both in the active and passive categories. In most applications, an absorber is placed on the primary structure at the point where vibration is most problematic. We are talking about a collocated absorber. However, often the parts of the structure affected by vibration are difficult to access. For example, we cannot place an active vibration absorber at the tip of a cutting tool during machining or at the end point of a micromanipulator on a surgical robot. Therefore, it is highly desirable to perform vibration suppression using a non-collocated absorber that is remote from the point where the suppression is required. Passive vibration absorber on a primary structure has been used for several decades [7]. From the more recent literature, we can mention the passively tuned multi-degree-of-freedom absorber [8] or the use of two passive absorbers with one-degree-of-freedom (DOF) [9]. In [10], multiple passive absorbers are tuned for the primary and secondary mode shapes of a wind turbine to suppress vibration. In most applications, the absorbers are still considered as passive [11] or semi-passive [12]. They can reduce vibration significantly, but they cannot achieve complete suppression. To achieve this, the absorber must be changed to an ideal absorber that has zero damping and the natural frequency equal to the excitation frequency [13].

In the 1990s, research group of professor Nejat Olgac introduced the concept of delayed resonator (DR) [14, 15, 16], which performs exactly this task. It is an actively tuned absorber that uses time-delayed feedback from the position [17], acceleration [18] or velocity [19] of the absorber. The advantages of DR are simple implementation, complete vibration suppression for the tuned frequency and independence of the actuator parameters from the primary structure parameters. A complete stability analysis of a DR with lumped delay was performed in [20]. The analysis shows some negative effects when lumped-delayed feedback is taken from acceleration measurements. In order to mitigate this, an alternative "distributed-delay" resonator was proposed in [21]. Consequently, a modified DR [22] was proposed, where the acceleration based delayed feedback is supplemented by a non-delayed path in order to widen the stable suppression frequency range. Significant results have been achieved in the design of distributed delay DRs with enhanced robustness in [23] and [24] performed using spectrum optimization techniques. A systematic comparison of DRs with position, velocity and acceleration feedback with the focus on the robustness, stability and absorber design have been done in [25]. In [26], DRs targeting multiple frequencies were designed and analysed.

Recently, Olgac and Jenkins demonstrated that the DR is applicable for non-collocated vibration absorption of a system composed of a serial interconnection of flexibly linked masses [27], [28]. Note that the findings confirm the earlier results by Filipovic and Schröder presented in [29], where the non-collocated vibration suppression was performed by linear active resonators. Subsequently to Olgac and Jenkins, in [30], a generally applicable spectral design of non-collocated vibration suppression performed primarily by a DR is presented, and in [31], an output feedback controller is used to assign the active zero couple and to stabilize the system with feedback delay.

Also recently, an enhanced attention has been paid to extending the DR concept from one-dimensional to multi-dimensional vibration absorption. Following the conceptual design of the absorber [32] based on the 2D parallel mechanism, a 3DOF DR for planar

vibration absorption was proposed [33]. Subsequently, in [34] a thorough analysis and parameter optimization for the 2D-DR was performed. As a further step, a Stewart platform based 3D-DR with 6DOF was proposed and conceptually verified in [35]. It was shown that the required uni-frequency cannot be achieved by the classical DR feedback only. An additional correction feedback had to be introduced to gain the uni-frequency feature. This partially motivates research presented in this paper, where this necessity is overcome by considering a symmetric spatial resonator absorber. Note that so far, multi-dimensional DRs have been considered in the collocated deployment only. In this paper, the effects on vibration suppression by multi-dimensional DRs are studied for the first time from the viewpoint of non-collocated vibration suppression.Besides, in contrast to the article [35], the presented paper is devoted to a spatial 6 DOF active dynamically isotropic absorber in the situation where the primary structure is spatial and fully flexible. This is also considered for the base/connecting plates/walls of absorber device itself. New results for such a complex case of absorption are presented, some theoretical conclusions are formulated and the behaviour of a complex modally described flexible system for collocated absorption and non-collocated placement of a spatial absorber is shown.

The paper is organized as follows. Section 2 briefly describes the preliminaries for both the delayed resonator concept and the modal description of a flexible system. Section 3 is devoted to the novel form of a dynamically isotropic (unifrequency) spatial 6 DOF absorber. The subsequent Section 4 discusses the primary flexible structure. The structure-absorber connection is addressed in Section 5. In Section 6, theoretical conclusions regarding the collocation of the absorber connected to the flexible system are presented. The application of active delayed feedback for 6 DOF absorber is introduced in Section 7. Simulation experiments for both the collocated and the non-collocated deployment are given in Section 8. The conclusions are reached in Section 9.

2. Preliminaries

2.1. 1-DOF delayed resonator

Figure 1a) shows an active vibration absorber connected to the base body. The differential equation governing the absorber dynamics has the form

$$m_a \ddot{x}_a(t) + c_a \dot{x}_a(t) + k_a x_a(t) = u(t), \tag{1}$$

where x_a is absorber position, u is the control force input, m_a, k_a and c_a represent absorber mass, stiffness and damping. The goal is to absorb the vibrations of the primary body when excited by a harmonic force $f(t)$ with frequency ω. An ideal absorber that achieves this is shown in Figure 1b). Its dynamics equation is given by

$$m_a \ddot{x}_a(t) + k_{ideal} x_a(t) = 0. \tag{2}$$

Vibrations of the primary mass are completely absorbed when $\omega \to \omega_a = \sqrt{\frac{k_{ideal}}{m_a}}$. Consider positional feedback of the active absorber in the form

$$u(t) = g x_a(t - \tau), \tag{3}$$

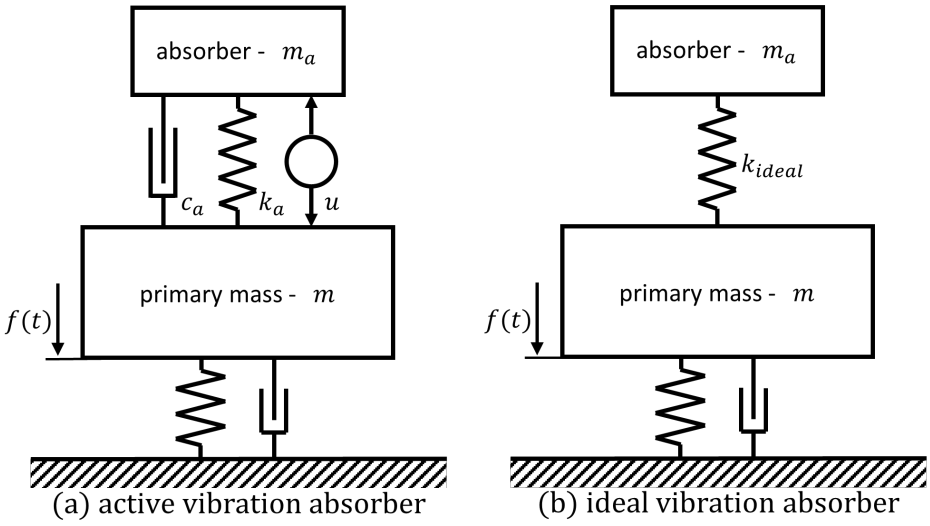


Figure 1: Active (a) and ideal (b) vibration absorber

where g is the gain and τ is the delay. Equations (1) and (2) can be rewritten in the frequency domain form

$$\left(-\omega^2 m_a + j\omega c_a + k_a - ge^{-j\omega\tau}\right) X_a\left(j\omega\right) = 0, \tag{4}$$

$$\left(-\omega^2 m_a + k_{ideal}\right) X_a\left(j\omega\right) = 0. \tag{5}$$

From the requirement of equal behaviour of active and ideal absorber at the frequency ω, we get the condition

$$ge^{-j\omega\tau} = j\omega c_a + k_a - k_{ideal}. \tag{6}$$

Solving the real and imaginary components separately implies the two solution sets: either

$$g = -\sqrt{\left(k_a - k_{ideal}\right)^2 + \left(\omega c_a\right)^2}, \tag{7}$$

$$\tau = \frac{1}{\omega}\left(\arctan\frac{\omega c_a}{k_{ideal} - k_a} + 2\left(\kappa - 1\right)\pi\right), \kappa = 1, 2, ... \tag{8}$$

or

$$g = \sqrt{\left(k_a - k_{ideal}\right)^2 + \left(\omega c_a\right)^2}, \tag{9}$$

$$\tau = \frac{1}{\omega}\left(\arctan\frac{\omega c_a}{k_{ideal} - k_a} + \left(2\kappa - 1\right)\pi\right), \kappa = 1, 2, ... \tag{10}$$

where κ is the branch number. As shown in [25], the best stability and robustness characteristics are obtained for the smallest possible delay τ. Therefore, the solution set (7)-(8) with $\kappa = 1$ should be preferred. If the gain and delay meet these conditions, the active absorber behaves as the ideal one and the vibration is completely absorbed.

2.2. Description of the flexible structure using modal coordinates

A mechanical system is usually described by a differential equation of the form

$$\bar{\mathbf{M}}\ddot{\mathbf{x}} + \bar{\mathbf{B}}\dot{\mathbf{x}} + \bar{\mathbf{K}}\mathbf{x} = \mathbf{f}, \tag{11}$$

where $\bar{\mathbf{M}}$, $\bar{\mathbf{B}}$, $\bar{\mathbf{K}}$ are the mass, damping and stiffness matrices, $\mathbf{x}$ is a vector of physical coordinates and $\mathbf{f}$ represents the load. Using the modal transformation $\mathbf{x} = \mathbf{V}\mathbf{q}$, with $\mathbf{q}$ the vector of modal coordinates and $\mathbf{V}$ the modal matrix, the equation (11) can be rewritten as

$$\mathbf{V}^T\bar{\mathbf{M}}\mathbf{V}\ddot{\mathbf{q}} + \mathbf{V}^T\bar{\mathbf{B}}\mathbf{V}\dot{\mathbf{q}} + \mathbf{V}^T\bar{\mathbf{K}}\mathbf{V}\mathbf{q} = \mathbf{V}^T\mathbf{f}. \tag{12}$$

The modal matrix $\mathbf{V}$ is composed of the eigenmodes of the system corresponding to non-zero eigenfrequencies and is normalized by the mass matrix according to the relation

$$\mathbf{V}^T\bar{\mathbf{M}}\mathbf{V} = \mathbf{I}. \tag{13}$$

Using the last term on the left-hand side of equation (12), we can define the diagonal matrix of natural frequencies of the system Ω as

$$\mathbf{V}^T\bar{\mathbf{K}}\mathbf{V} = \Omega^2. \tag{14}$$

If we consider proportional damping, we can also diagonalise the velocity term as

$$\mathbf{V}^T\bar{\mathbf{B}}\mathbf{V} = 2\mathbf{b}_r\Omega, \tag{15}$$

where $\mathbf{b}_r$ is the diagonal matrix of the proportional damping of each mode. Equation (12) is then rewritten in the form

$$\ddot{\mathbf{q}} + 2\mathbf{b}_r\Omega\dot{\mathbf{q}} + \Omega^2\mathbf{q} = \mathbf{V}^T\mathbf{f}, \tag{16}$$

which represents N independent differential equations, where N is the number of modes.

2.3. State-space representation

If we use modal coordinates to create a state-space model, it is advisable to define the state vector in such a way as to obtain the model in an almost-balanced form that is advantageous for both reduction and computational complexity. The state vector $\mathbf{z}$ for such a model is as follows

$$\mathbf{z} = \begin{bmatrix} \Omega_1 q_1 & \dot{q}_1 & \Omega_2 q_2 & \dot{q}_2 & \dots & \Omega_N q_N & \dot{q}_N \end{bmatrix}^T. \tag{17}$$

We then obtain a block-diagonal system matrix

$$\bar{\mathbf{A}} = \begin{bmatrix} 0 & \Omega_1 & \dots & 0 & 0 \\ -\Omega_1 & -2b_{r1}\Omega_1 & \dots & 0 & 0 \\ \dots & \dots & \dots & \dots & \dots \\ 0 & 0 & \dots & 0 & \Omega_N \\ 0 & 0 & \dots & -\Omega_N & -2b_{rN}\Omega_N \end{bmatrix}. \tag{18}$$

and an input matrix

$$\bar{\mathbf{B}} = \begin{bmatrix} \mathbf{0} & \mathbf{V}_1 & \mathbf{0} & \mathbf{V}_2 & \dots & \mathbf{0} & \mathbf{V}_N \end{bmatrix}^T. \tag{19}$$

The whole system can be described by the well-known equations

$$\dot{\mathbf{z}} = \bar{\mathbf{A}}\mathbf{z} + \bar{\mathbf{B}}\mathbf{f} \tag{20}$$

$$\mathbf{y} = \bar{\mathbf{C}}\mathbf{z} + \bar{\mathbf{D}}\mathbf{f}, \tag{21}$$

with the input vector $\mathbf{f}$ and outputs $\mathbf{y}$ selected as required. Position, velocity and acceleration are the most commonly used output measurements and can be derived from a modal description of the mechanical system. In the case where a position output is considered

$$\mathbf{y} = \mathbf{x} = \mathbf{V}\mathbf{q} = \begin{bmatrix} \frac{\mathbf{V}_1}{\Omega_1} & \mathbf{0} & \frac{\mathbf{V}_2}{\Omega_2} & \mathbf{0} & \dots & \frac{\mathbf{V}_N}{\Omega_N} & \mathbf{0} \end{bmatrix} \mathbf{z} \tag{22}$$

and therefore

$$\mathbf{C}_{POS} = \begin{bmatrix} \frac{\mathbf{V}_1}{\Omega_1} & \mathbf{0} & \frac{\mathbf{V}_2}{\Omega_2} & \mathbf{0} & \dots & \frac{\mathbf{V}_N}{\Omega_N} & \mathbf{0} \end{bmatrix}, \tag{23}$$

$$\mathbf{D}_{POS} = \mathbf{0}. \tag{24}$$

In the case of a velocity output

$$\mathbf{y} = \dot{\mathbf{x}} = \mathbf{V}\dot{\mathbf{q}} = \begin{bmatrix} \mathbf{0} & \mathbf{V}_1 & \mathbf{0} & \mathbf{V}_2 & \dots & \mathbf{0} & \mathbf{V}_N \end{bmatrix} \mathbf{z} \tag{25}$$

and

$$\mathbf{C}_{VEL} = \begin{bmatrix} \mathbf{0} & \mathbf{V}_1 & \mathbf{0} & \mathbf{V}_2 & \dots & \mathbf{0} & \mathbf{V}_N \end{bmatrix}, \tag{26}$$

$$\mathbf{D}_{VEL} = \mathbf{0}. \tag{27}$$

To express the acceleration it is necessary to use differential equation (16) and substitute into the relation

$$\mathbf{y} = \ddot{\mathbf{x}} = \mathbf{V}\ddot{\mathbf{q}} = -2\mathbf{V}\mathbf{b}_r\Omega\dot{\mathbf{q}} - \mathbf{V}\Omega^2\mathbf{q} + \mathbf{V}\mathbf{V}^T\mathbf{f}. \tag{28}$$

Hence, the acceleration can be expressed as

$$\ddot{\mathbf{x}} = \begin{bmatrix} -\mathbf{V}_1\Omega_1 & -2\mathbf{V}_1 b_{r1}\Omega_1 & \dots & -\mathbf{V}_N\Omega_N & -2\mathbf{V}_N b_{rN}\Omega_N \end{bmatrix} \mathbf{z} + \left(\sum_{i=1}^{N} \mathbf{V}_i \mathbf{V}_i^T \right) \mathbf{f} \tag{29}$$

and the output and the feedforward matrices are defined as

$$\mathbf{C}_{ACC} = \begin{bmatrix} -\mathbf{V}_1\Omega_1 & -2\mathbf{V}_1 b_{r1}\Omega_1 & \dots & -\mathbf{V}_N\Omega_N & -2\mathbf{V}_N b_{rN}\Omega_N \end{bmatrix}, \tag{30}$$

$$\mathbf{D}_{ACC} = \left[\sum_{i=1}^{N} \mathbf{V}_i \mathbf{V}_i^T \right]. \tag{31}$$

2.4. Model reduction

The accuracy of a dynamic model is often closely related to its size. For example, a model obtained by the finite element method usually contains a large number of degrees of freedom. This complexity increases the computational complexity of the simulation. It is therefore advisable to reduce such a model with respect to the properties under consideration [36].

Assume that we want to reduce the state model by restricting to certain modes and omitting the natural frequencies outside the desired band. The system matrix is considered in the form

$$\bar{\mathbf{A}} = \begin{bmatrix} \mathbf{A}_{11} & \mathbf{A}_{12} \\ \mathbf{A}_{21} & \mathbf{A}_{22} \end{bmatrix}, \tag{32}$$

where the eigenvalues of $\mathbf{A_{11}}$ correspond to n modes to be preserved. The matrices of the state-space representation can be partitioned accordingly as

$$SS_{orig} = \begin{bmatrix} \bar{\mathbf{A}} & \bar{\mathbf{B}} \\ \bar{\mathbf{C}} & \bar{\mathbf{D}} \end{bmatrix} = \begin{bmatrix} \mathbf{A}_{11} & \mathbf{A}_{12} & \mathbf{B}_1 \\ \mathbf{A}_{21} & \mathbf{A}_{22} & \mathbf{B}_2 \\ \mathbf{C}_1 & \mathbf{C}_2 & \bar{\mathbf{D}} \end{bmatrix}. \tag{33}$$

The simplest way of reduction, known as modal truncation, would be to omit those parts that lie outside the desired frequency range. The reduced system would then be described by the matrices

$$SS_{red} = \begin{bmatrix} \mathbf{A}_{11} & \mathbf{B}_1 \\ \mathbf{C}_1 & \bar{\mathbf{D}} \end{bmatrix}. \tag{34}$$

Such a reduction, however, usually does not capture the original system in the best way, especially at low frequencies and low levels of approximation. In contrast, the singular perturbation approximation (SPA) [37] is a reduction method with residual that statically takes into account the omitted states. The system reduced with the residual is described by matrices

$$SS_{spa} = \begin{bmatrix} \mathbf{A}_{11} - \mathbf{A}_{12}\mathbf{A}_{22}^{-1}\mathbf{A}_{21} & \mathbf{B}_1 - \mathbf{A}_{12}\mathbf{A}_{22}^{-1}\mathbf{B}_2 \\ \mathbf{C}_1 - \mathbf{C}_2\mathbf{A}_{22}^{-1}\mathbf{A}_{21} & \bar{\mathbf{D}} - \mathbf{C}_2\mathbf{A}_{22}^{-1}\mathbf{B}_2 \end{bmatrix}. \tag{35}$$

Since $\mathbf{A}_{12} = \mathbf{0}$ and $\mathbf{A}_{21} = \mathbf{0}$, see (18), the description can be further simplified

$$SS_{MODALspa} = \begin{bmatrix} \mathbf{A}_{11} & \mathbf{B}_1 \\ \mathbf{C}_1 & \bar{\mathbf{D}} - \mathbf{C}_2\mathbf{A}_{22}^{-1}\mathbf{B}_2 \end{bmatrix}. \tag{36}$$

The resulting matrix description differs from the simple reduction (34) only in the feedthrough matrix $\mathbf{D}$. Moreover, matrix $\mathbf{A}_{22}$ can be easily expressed analytically thanks to the chosen modal description, which is beneficial considering the high number of degrees of freedom of the original system and the computational complexity of matrix inversion. The position feedforward matrix changes to

$$\mathbf{D}_{POS,SPA} = \sum_{i=n+1}^{N} \frac{\mathbf{V}_i \mathbf{V}_i^T}{\Omega_i^2} = \mathbf{G} - \sum_{j=1}^{n} \frac{\mathbf{V}_j \mathbf{V}_j^T}{\Omega_j^2}, \tag{37}$$

where $\mathbf{G} = \mathbf{K}^{-1}$ [36]. The simplification on the right hand side allows to use only the reduced system eigenmodes of number n instead of all N eigenmodes of the original large system.

3. Absorption of spatial structure vibrations

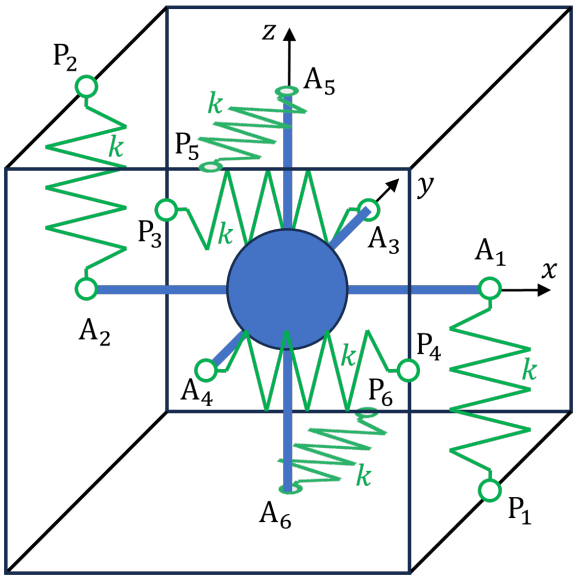


Figure 2: Ideal unifrequency spatial vibration absorber

The aim is to design an absorber that will suppress the vibration of the primary structure in all directions, i.e. in 3 sliding and 3 rotational, and ideally be able to do this passively, without active control intervention. The initial structure considered for the ideal absorber is shown in Figure 2. It is a rigid spatial cross that is connected to the flexible primary structure at 6 points P_i, the damping in the springs is neglected for the ideal absorber, the points on the absorber A_i lie on the surface of the sphere centered at the center of gravity of the absorber with radius R. The absorber has four parameters: the mass m, the stiffness of the springs k, the coordinates of the location of the spring attachment from the centre of gravity R, and the moment of inertia I. Relations between the absorber parameters will be derived later on from the requirement to tune the absorber to a single frequency. The springs have free length L.

3.1. Dynamic model

The general position of the absorber in space is described by coordinates $x_a, y_a, z_a, \varphi_x, \varphi_y, \varphi_z$. The total transformation matrix can then be expressed in the form

$$\mathbf{T} = \mathbf{T}_x(x_a)\mathbf{T}_y(y_a)\mathbf{T}_z(z_a)\mathbf{T}_{\varphi_x}(\varphi_x)\mathbf{T}_{\varphi_y}(\varphi_y)\mathbf{T}_{\varphi_z}(\varphi_z), \tag{38}$$

where $\mathbf{T}_{\cdot}(.)$ are transformation matrices of basic motions [38]. Since we assume small vibrations and therefore small rotation angles of the absorber, we can consider $\sin\varphi \approx \varphi$, $\cos\varphi \approx 1$, $\sin^2\varphi \approx 0$ and $\cos^2\varphi \approx 1$, which leads to a simplification of matrix $\mathbf{T}$ into

transformation matrix $\mathbf{T}_a$ (40)

$$\mathbf{T} = \begin{bmatrix} \cos\varphi_y \cos\varphi_z & -\cos\varphi_y \sin\varphi_z & \sin\varphi_y & x_a \\ \cos\varphi_x \sin\varphi_z + \cos\varphi_z \sin\varphi_x \sin\varphi_y & \cos\varphi_x \cos\varphi_z - \sin\varphi_x \sin\varphi_y \sin\varphi_z & -\cos\varphi_y \sin\varphi_x & y_a \\ \sin\varphi_x \sin\varphi_z - \cos\varphi_x \cos\varphi_z \sin\varphi_y & \cos\varphi_z \sin\varphi_x + \cos\varphi_x \sin\varphi_y \sin\varphi_z & \cos\varphi_y \cos\varphi_x & z_a \\ 0 & 0 & 0 & 1 \end{bmatrix} \tag{39}$$

$$\mathbf{T}_a = \begin{bmatrix} 1 & -\varphi_z & \varphi_y & x_a \\ \varphi_z & 1 & -\varphi_x & y_a \\ -\varphi_y & \varphi_x & 1 & z_a \\ 0 & 0 & 0 & 1 \end{bmatrix} \tag{40}$$

The extended radius vector of the point position change $\Delta\mathbf{r}_{A_i} = [\Delta x_{A_i}, \Delta y_{A_i}, \Delta z_{A_i}, 1]^T$ can be described as

$$\Delta\mathbf{r}_{A_i} = \mathbf{T}_a\mathbf{r}_{A_i} - \mathbf{r}_{A_i} = (\mathbf{T}_a - \mathbf{I})\,\mathbf{r}_{A_i} = \begin{bmatrix} 0 & -\varphi_z & \varphi_y & x_a \\ \varphi_z & 0 & -\varphi_x & y_a \\ -\varphi_y & \varphi_x & 0 & z_a \\ 0 & 0 & 0 & 0 \end{bmatrix} \begin{bmatrix} x_{A_i} \\ y_{A_i} \\ z_{A_i} \\ 1 \end{bmatrix}. \tag{41}$$

Forces in points A_i can be calculated using the spring stiffness as

$$F_i = k \begin{bmatrix} \Delta x_{A_i} - x_{P_i} \\ \Delta y_{A_i} - y_{P_i} \\ \Delta z_{A_i} - z_{P_i} \end{bmatrix} \cdot \mathbf{e}_i, \tag{42}$$

where $x_{P_i}, y_{P_i}, z_{P_i}$ are the coordinates of the absorber connection point to the system, P_i. These positions are obtained from the dynamic model of the system. Vector $\mathbf{e}_i$ is the unit vector in the direction of the axis in which the force acts, since we consider small deflections and therefore the deflection of the spring from the direction of the coordinate axes can be considered negligible. For example, the radius vector of point A_1 is

$$\Delta\mathbf{r}_{A_1} = \begin{bmatrix} \Delta x_{A_1} \\ \Delta y_{A_1} \\ \Delta z_{A_1} \\ 1 \end{bmatrix} = \begin{bmatrix} 0 & -\varphi_z & \varphi_y & x_a \\ \varphi_z & 0 & -\varphi_x & y_a \\ -\varphi_y & \varphi_x & 0 & z_a \\ 0 & 0 & 0 & 0 \end{bmatrix} \begin{bmatrix} R \\ 0 \\ 0 \\ 1 \end{bmatrix} = \begin{bmatrix} x_a \\ y_a + R\varphi_z \\ z_a - R\varphi_y \\ 1 \end{bmatrix} \tag{43}$$

and the force in A_1 is

$$F_1 = k \begin{bmatrix} x_a - x_{P_1} \\ y_a + R\varphi_z - y_{P_1} \\ z_a - R\varphi_y - z_{P_1} \end{bmatrix} \cdot \begin{bmatrix} 0 \\ 0 \\ 1 \end{bmatrix} = k\,(z_a - R\varphi_y - z_{P_1})\,. \tag{44}$$

Repeating the same procedure for the other pairs of points A_i, P_i we obtain the forces:

$$F_2 = k\,(z_a + R\varphi_y - z_{P_2}) \tag{45}$$

$$F_3 = k\,(x_a - R\varphi_z - x_{P_3}) \tag{46}$$

$$F_4 = k\left(x_a + R\varphi_z - x_{P_4}\right) \tag{47}$$

$$F_5 = k\left(y_a - R\varphi_x - y_{P_5}\right) \tag{48}$$

$$F_6 = k\left(y_a + R\varphi_x - y_{P_6}\right) \tag{49}$$

Using the knowledge of the forces acting on the absorber, we can formulate the equations of motion of the absorber in the compact form

$$\mathbf{M}\ddot{\mathbf{X}}_a = f\left(\mathbf{X}_a, \mathbf{X}_p\right), \tag{50}$$

where

$$\mathbf{X}_a = [x_a, y_a, z_a, \varphi_x, \varphi_y, \varphi_z]^T, \tag{51}$$

$$\mathbf{X}_p = [z_{P_1}, z_{P_2}, x_{P_3}, x_{P_4}, y_{P_5}, y_{P_6}]^T, \tag{52}$$

$$\mathbf{M} = \begin{bmatrix} m & 0 & 0 & 0 & 0 & 0 \\ 0 & m & 0 & 0 & 0 & 0 \\ 0 & 0 & m & 0 & 0 & 0 \\ 0 & 0 & 0 & I & 0 & 0 \\ 0 & 0 & 0 & 0 & I & 0 \\ 0 & 0 & 0 & 0 & 0 & I \end{bmatrix}. \tag{53}$$

The right-hand side of (50) can be expressed as

$$f\left(\mathbf{X}_a, \mathbf{X}_p\right) = \begin{bmatrix} -k\left(x_a - R\varphi_z - x_{P_3}\right) - k\left(x_a + R\varphi_z - x_{P_4}\right) \\ -k\left(y_a - R\varphi_x - y_{P_5}\right) - k\left(y_a + R\varphi_x - y_{P_6}\right) \\ -k\left(z_a - R\varphi_y - z_{P_1}\right) - k\left(z_a + R\varphi_y - z_{P_2}\right) \\ k\left(y_a - R\varphi_x - y_{P_5}\right) R - k\left(y_a + R\varphi_x - y_{P_6}\right) R \\ k\left(z_a - R\varphi_y - z_{P_1}\right) R - k\left(z_a + R\varphi_y - z_{P_2}\right) R \\ k\left(x_a - R\varphi_z - x_{P_3}\right) R - k\left(x_a + R\varphi_z - x_{P_4}\right) R \end{bmatrix}. \tag{54}$$

Rewritten in matrix form we get

$$\mathbf{M}\ddot{\mathbf{X}}_a = -\mathbf{K}\mathbf{X}_a - \mathbf{K}_p\mathbf{X}_p, \tag{55}$$

where

$$\mathbf{K} = \begin{bmatrix} 2k & 0 & 0 & 0 & 0 & 0 \\ 0 & 2k & 0 & 0 & 0 & 0 \\ 0 & 0 & 2k & 0 & 0 & 0 \\ 0 & 0 & 0 & 2kR^2 & 0 & 0 \\ 0 & 0 & 0 & 0 & 2kR^2 & 0 \\ 0 & 0 & 0 & 0 & 0 & 2kR^2 \end{bmatrix}, \tag{56}$$

$$\mathbf{K}_p = \begin{bmatrix} 0 & 0 & -k & -k & 0 & 0 \\ 0 & 0 & 0 & 0 & -k & -k \\ -k & -k & 0 & 0 & 0 & 0 \\ 0 & 0 & 0 & 0 & kR & -kR \\ kR & -kR & 0 & 0 & 0 & 0 \\ 0 & 0 & kR & -kR & 0 & 0 \end{bmatrix}. \tag{57}$$

3.2. Unifrequency absorber

The goal is to adjust the absorber parameters m, k, R, I so that the absorber has all natural frequencies identical. Such an absorber is called a unifrequency absorber. The dynamics of the ideal spatial absorber according to the Figure 2 is described by the equation

$$\mathbf{M}\ddot{\mathbf{X}}_a + \mathbf{K}\mathbf{X}_a = 0 \tag{58}$$

and in the Laplace form

$$\left(s^2\mathbf{M} + \mathbf{K}\right)\mathbf{X}_a\left(s\right) = 0. \tag{59}$$

The mass matrix $\mathbf{M}$ and the stiffness matrix $\mathbf{K}$ are diagonal. The matrix system therefore splits into 6 independent equations. The condition for the relationship between the absorber parameters is obtained by solving these 6 independent equations. The first 3 equations are identical

$$ms^2 + 2k = 0 \tag{60}$$

The natural frequencies from (60) are

$$\Omega_{1,2,3} = \sqrt{\frac{2k}{m}}. \tag{61}$$

The remaining 3 equations are also identical

$$Is^2 + 2kR^2 = 0 \tag{62}$$

with natural frequencies obtained as

$$\Omega_{4,5,6} = \sqrt{\frac{2kR^2}{I}}. \tag{63}$$

The necessary condition of the unifrequency absorber is the equality of the natural frequencies $\Omega_{1,2,3}$ and $\Omega_{4,5,6}$. Considering the equality

$$\Omega_{1,2,3} = \Omega_{4,5,6} \tag{64}$$

implies the structural constraint

$$I = mR^2. \tag{65}$$

Thus, the parameters m, k, I and R must be set to satisfy equation (64) with respect to the arbitrary selected natural frequency of the absorber.

4. Primary structure

As a model example of a spatial compliant primary structure whose vibrations we want to suppress, a flexible frame with many degrees of freedom was used. The aim was to test the methodology on a model of arbitrary real flexible structure of large scale, for which a modal model of an anonymized steel structure provided by an engineering company was used. The original FEM model used by this industrial company has 315852 elements and 614 193 nodes. The provided modal model contains 50 eigenmodes corresponding

to the lowest 50 eigenfrequencies summarized in Table 1. The overall dimensions of the frame are - length 12400 mm, width 3900 mm, height 1020 mm and the total weight of the frame with the installed equipment is 123300 kg. The frame is welded from 20 mm and 40 mm thick plates in combination with HEB profiles, which are made from 1.0038+N steel. The frame is supported by eight spring elements with viscous dampers. For the model outputs only 189 selected coordinates from eigenmodes have been used for vibration description of 63 important points. Important points are indicated in the simplified diagram in Figure 3. Point F is the location of the excitation by the periodic force and the point whose vibration we want to suppress is indicated N. Points S_i and S_j represent two of 39 considered absorber locations, see Figure 7 and Figure 8. The points Q_j are relevant to describe the position of the absorber on the primary mass and their meaning will be explained in the next section.

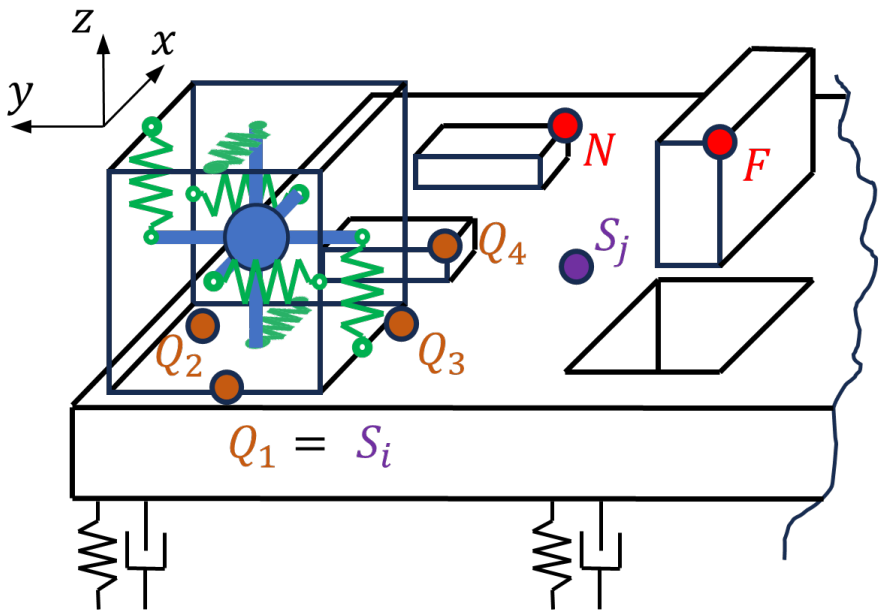


Figure 3: Scheme of the absorber location on the primary mass with important points indicated

The dynamical model has been created in modal coordinates according to Section 2.2 and converted to state-space representation as described in Section 2.3 with respect to possible easy reduction of the system complexity. The model considers the first 50 natural frequencies of the structure, see Table 1, and the corresponding eigenmodes normalized according to the mass matrix (13) with the proportional damping model (15) where each eigenmode is assigned a proportional damping.

Table 1: Lowest eigenfrequencies of the primary structure [rad/s]

Ω_1	Ω_2	Ω_3	Ω_4	Ω_5	Ω_6	Ω_7	Ω_8	Ω_9	Ω_{10}
3.941	4.717	5.248	6.133	6.747	7.199	7.882	9.539	11.180	12.117
Ω_{11}	Ω_{12}	Ω_{13}	Ω_{14}	Ω_{15}	Ω_{16}	Ω_{17}	Ω_{18}	Ω_{19}	Ω_{20}
13.144	14.475	16.539	17.155	18.462	24.519	25.844	26.265	28.469	29.359
Ω_{21}	Ω_{22}	Ω_{23}	Ω_{24}	Ω_{25}	Ω_{26}	Ω_{27}	Ω_{28}	Ω_{29}	Ω_{30}
30.068	30.774	33.299	33.796	36.948	37.228	40.637	44.298	44.938	47.209
Ω_{31}	Ω_{32}	Ω_{33}	Ω_{34}	Ω_{35}	Ω_{36}	Ω_{37}	Ω_{38}	Ω_{39}	Ω_{40}
49.021	51.486	52.059	53.840	54.342	55.444	55.987	56.982	60.961	62.582
Ω_{41}	Ω_{42}	Ω_{43}	Ω_{44}	Ω_{45}	Ω_{46}	Ω_{47}	Ω_{48}	Ω_{49}	Ω_{50}
63.831	64.863	66.684	70.346	76.083	76.583	80.620	82.130	83.079	83.967

5. Connection of the absorber to the primary structure

Figure 3 shows the approximate location of the absorber on the primary structure. The problem is that the absorber connection points are not within the 63 points that describe the behaviour of the flexible frame. Therefore, the connection points must be defined using existing points to match the flexible behaviour of the system.

The behaviour of the absorber connected to the system through the points P_i is governed by the differential equation (55), which can be re-written in Laplace form as

$$s^2\mathbf{M}\mathbf{X}_a(s) = -\mathbf{K}\mathbf{X}_a(s) - \mathbf{K}_p\mathbf{X}_p(s). \tag{66}$$

The transfer function between the absorber coordinates $\mathbf{X}_a$ and the coordinates of the connection points $\mathbf{X}_p$ can be expressed as

$$\mathbf{X}_a(s) = \mathbf{G}_a(s)\,\mathbf{X}_p(s), \tag{67}$$

where

$$\mathbf{G}_a(s) = -\left(s^2\mathbf{M} + \mathbf{K}_a\right)^{-1}\mathbf{K}_p. \tag{68}$$

The coordinates $\mathbf{X}_p$ need to be expressed using the state coordinates in which the primary system is modelled in order to connect the absorber model to the primary structure model. We use 4 non-planar points Q_i of the primary structure to express coordinates of P_i points as linear combination. We define the rotation matrix $\mathbf{R}$ that

$$\begin{bmatrix} x_{Q2}-x_{Q1} & x_{Q3}-x_{Q1} & x_{Q4}-x_{Q1} \\ y_{Q2}-y_{Q1} & y_{Q3}-y_{Q1} & y_{Q4}-y_{Q1} \\ z_{Q2}-z_{Q1} & z_{Q3}-z_{Q1} & z_{Q4}-z_{Q1} \end{bmatrix} = \mathbf{R}\begin{bmatrix} x_{Q2l}-x_{Q1l} & x_{Q3l}-x_{Q1l} & x_{Q4l}-x_{Q1l} \\ y_{Q2l}-y_{Q1l} & y_{Q3l}-y_{Q1l} & y_{Q4l}-y_{Q1l} \\ z_{Q2l}-z_{Q1l} & z_{Q3l}-z_{Q1l} & z_{Q4l}-z_{Q1l} \end{bmatrix}, \tag{69}$$

where on the left-hand side are the global coordinates and on the right-hand side the local coordinates of the points Q_i. The local coordinates are constant, so we can easily define

$$\mathbf{R} = \begin{bmatrix} x_{Q2}-x_{Q1} & x_{Q3}-x_{Q1} & x_{Q4}-x_{Q1} \\ y_{Q2}-y_{Q1} & y_{Q3}-y_{Q1} & y_{Q4}-y_{Q1} \\ z_{Q2}-z_{Q1} & z_{Q3}-z_{Q1} & z_{Q4}-z_{Q1} \end{bmatrix}\begin{bmatrix} x_{Q2l}-x_{Q1l} & x_{Q3l}-x_{Q1l} & x_{Q4l}-x_{Q1l} \\ y_{Q2l}-y_{Q1l} & y_{Q3l}-y_{Q1l} & y_{Q4l}-y_{Q1l} \\ z_{Q2l}-z_{Q1l} & z_{Q3l}-z_{Q1l} & z_{Q4l}-z_{Q1l} \end{bmatrix}^{-1} \tag{70}$$

and

$$P_i = Q_1 + \mathbf{R}\left[P_{ixl}, P_{iyl}, P_{izl}\right]^T, \tag{71}$$

where P_{ixl}, P_{iyl} and P_{izl} are the local coordinates, i.e. dimensions, of the absorber. Specifically

$$P_1 = Q_1 \tag{72}$$

$$P_2 = Q_1 + \mathbf{R}\left[-2R, 0, 2L\right]^T \tag{73}$$

$$P_3 = Q_1 + \mathbf{R}\left[-R - L, R, L\right]^T \tag{74}$$

$$P_4 = Q_1 + \mathbf{R}\left[-R + L, -R, L\right]^T \tag{75}$$

$$P_5 = Q_1 + \mathbf{R}\left[-R, -L, L + R\right]^T \tag{76}$$

$$P_6 = Q_1 + \mathbf{R}\left[-R, L, L - R\right]^T. \tag{77}$$

Considering the Laplace transform of the state-space model (20)-(21), namely its reduced part as described in (32)-(36), and expressing the connected absorber as an applied external force, we arrive to

$$s\mathbf{Z}\left(s\right) = \mathbf{A}\mathbf{Z}\left(s\right) + \mathbf{B}_{\mathrm{F}}\mathrm{F}\left(s\right) + \mathbf{B}_{\mathrm{P}}\left(\mathbf{S}_1\mathbf{X}_a\left(s\right) + \mathbf{S}_2\mathbf{X}_p\left(s\right)\right), \tag{78}$$

$$\mathbf{X}\left(s\right) = \mathbf{C}\mathbf{Z}\left(s\right) + \mathbf{D}_{\mathrm{F}}\mathrm{F}\left(s\right), \tag{79}$$

where $\mathbf{A} = \mathbf{A}_{11}$ from (32) is the $2n \times 2n$ matrix of the reduced system, $\mathbf{Z}\left(s\right)$ represents the state vector of the reduced system defined as the first $2n$ elements of $\mathbf{z}$ from(17), $\mathbf{X}\left(s\right)$ is the vector of 189 coordinates of 63 selected important points, $\mathbf{C}$ is the corresponding output matrix. Matrices $\mathbf{B}_{\mathrm{F}}$ and $\mathbf{D}_{\mathrm{F}}$ project the external excitation load by ω-harmonic force $\mathrm{F}\left(s\right)$ acting in the direction defined by the unity vector $\mathbf{e} = [e_x, e_y, e_z]^T$ at point F. The $\mathbf{B}_{\mathrm{P}}$ matrix projects forces from the absorber through the P_i points to the primary structure. The $\mathbf{B}_{\mathrm{P}}$ matrix is based on expressing P_i points coordinates using a combination of Q_i point coordinates (72) - (77). Matrices $\mathbf{S}_1$ and $\mathbf{S}_2$ are the stiffness matrices of the attached absorber

$$\mathbf{S}_1 = \begin{bmatrix} 0 & 0 & k & 0 & -kR & 0 \\ 0 & 0 & k & 0 & kR & 0 \\ k & 0 & 0 & 0 & 0 & -kR \\ k & 0 & 0 & 0 & 0 & kR \\ 0 & k & 0 & -kR & 0 & 0 \\ 0 & k & 0 & kR & 0 & 0 \end{bmatrix}, \tag{80}$$

$$\mathbf{S}_2 = \begin{bmatrix} -k & 0 & 0 & 0 & 0 & 0 \\ 0 & -k & 0 & 0 & 0 & 0 \\ 0 & 0 & -k & 0 & 0 & 0 \\ 0 & 0 & 0 & -k & 0 & 0 \\ 0 & 0 & 0 & 0 & -k & 0 \\ 0 & 0 & 0 & 0 & 0 & -k \end{bmatrix}. \tag{81}$$

Relations (72) to (77) represent 18 equations for all coordinates of the P_i points including the required coordinates of the $\mathbf{X}_p$ vector. As the contained coordinates of Q_i are the outputs of the system, we can define the matrix $\mathbf{C}_{abs}$ such that

$$\mathbf{X}_p = \mathbf{C}_{abs}\mathbf{Z}\left(s\right). \tag{82}$$

Equation (79) can be used to express the transfer from the force acting on the primary structure to the position of the primary structure points

$$\mathbf{X}\left(s\right) = \mathbf{G}_{\mathrm{X}}\left(s\right)\mathrm{F}\left(s\right), \tag{83}$$

where

$$\mathbf{G}_{\mathrm{X}}\left(s\right) = \mathbf{C}\left\{s\mathbf{I} - \mathbf{A} - \mathbf{B}_{\mathrm{P}}\left[-\mathbf{S}_1\left(s^2\mathbf{M} + \mathbf{K}\right)^{-1}\mathbf{K}_p + \mathbf{S}_2\right]\mathbf{C}_{abs}\right\}^{-1}\mathbf{B}_{\mathrm{F}}. \tag{84}$$

However, this formulation is not very suitable for numerical solutions. It is more practical to combine (66), (78) and (82) and consider further the following representation of the interconnection of the primary structure and the absorber:

$$\begin{bmatrix} s\mathbf{I} - \mathbf{A} - \mathbf{B}_{\mathrm{P}}\mathbf{S}_2\mathbf{C}_{abs} & -\mathbf{B}_{\mathrm{P}}\mathbf{S}_1 \\ \mathbf{K}_p\mathbf{C}_{abs} & s^2\mathbf{M} + \mathbf{K} \end{bmatrix}\begin{bmatrix} \mathbf{Z}\left(s\right) \\ \mathbf{X}_a\left(s\right) \end{bmatrix} = \begin{bmatrix} \mathbf{B}_{\mathrm{F}}\mathrm{F}\left(s\right) \\ \mathbf{0} \end{bmatrix}. \tag{85}$$

6. Collocated vibration absorption for an harmonic excitation force

In the collocated vibration absorption case, the absorber is located at the position where the vibrations are to be suppressed. The excitation force acts at a different location on the primary structure. Substituting (68) into (78) gives

$$\left(s\mathbf{I} - \mathbf{A}\right)\mathbf{Z}\left(s\right) - \mathbf{B}_{\mathrm{P}}\left[-\mathbf{S}_1\left(s^2\mathbf{M} + \mathbf{K}\right)^{-1}\mathbf{K}_p + \mathbf{S}_2\right]\mathbf{X}_p\left(s\right) = \mathbf{B}_{\mathrm{F}}\mathrm{F}\left(s\right). \tag{86}$$

Consider

$$\mathbf{H} = \left[\left(\mathbf{B}_{\mathrm{P}}\right)^T\left(\mathbf{B}_{\mathrm{P}}\right)\right]^{-1}\left(\mathbf{B}_{\mathrm{P}}\right)^T \tag{87}$$

and multiply (86) by the matrix $\mathbf{H}$ from the left, then

$$\mathbf{H}\left(s\mathbf{I} - \mathbf{A}\right)\mathbf{Z}\left(s\right) - \left[-\mathbf{S}_1\left(s^2\mathbf{M} + \mathbf{K}\right)^{-1}\mathbf{K}_p + \mathbf{S}_2\right]\mathbf{X}_p\left(s\right) = \mathbf{H}\mathbf{B}_{\mathrm{F}}\mathrm{F}\left(s\right). \tag{88}$$

The matrix $\mathbf{B}_{\mathrm{P}}$ must satisfy the condition

$$\left[\left(\mathbf{B}_{\mathrm{P}}\right)^T\left(\mathbf{B}_{\mathrm{P}}\right)\right]^{-1}\left(\mathbf{B}_{\mathrm{P}}\right)^T\left(\mathbf{B}_{\mathrm{P}}\right) = \mathbf{I} \tag{89}$$

which is fulfilled for the defined $\mathbf{B}_{\mathrm{P}}$.

Substitute $s = j\omega$ with ω being an arbitrary frequency and introduce the singular value decomposition

$$\left[-\mathbf{S}_1\left(\left(j\omega\right)^2\mathbf{M} + \mathbf{K}\right)^{-1}\mathbf{K}_p + \mathbf{S}_2\right] = \mathbf{U}\mathbf{\Sigma}\mathbf{V}, \tag{90}$$

where $\mathbf{U}$ and $\mathbf{V}$ are orthonormal matrices and

$$\mathbf{\Sigma} = \begin{bmatrix} \sigma_1 & 0 & 0 & 0 & 0 & 0 \\ 0 & \sigma_2 & 0 & 0 & 0 & 0 \\ 0 & 0 & \sigma_3 & 0 & 0 & 0 \\ 0 & 0 & 0 & \sigma_4 & 0 & 0 \\ 0 & 0 & 0 & 0 & \sigma_5 & 0 \\ 0 & 0 & 0 & 0 & 0 & \sigma_6 \end{bmatrix}. \tag{91}$$

The equation (88) can be rewritten as

$$\mathbf{H}\left(j\omega\mathbf{I} - \mathbf{A}\right)\mathbf{Z}\left(j\omega\right) - \mathbf{U}\mathbf{\Sigma}\mathbf{V}\mathbf{X}_p\left(j\omega\right) = \mathbf{H}\mathbf{B}_{\mathrm{F}}\mathrm{F}\left(j\omega\right) \tag{92}$$

or in the form

$$\mathbf{\Sigma}^{-1}\mathbf{U}^T\mathbf{H}\left(j\omega\mathbf{I} - \mathbf{A}\right)\mathbf{Z}\left(j\omega\right) - \mathbf{V}\mathbf{X}_p\left(j\omega\right) = \mathbf{\Sigma}^{-1}\mathbf{U}^T\mathbf{H}\mathbf{B}_{\mathrm{F}}\mathrm{F}\left(j\omega\right). \tag{93}$$

The unifrequency property means that all the singular numbers of $\mathbf{\Sigma}$ are identical and turns $\sigma_1 = \sigma_2 = \sigma_3 = \sigma_4 = \sigma_5 = \sigma_6 \to \infty$ for $\omega \to \omega_a = \Omega_{1,2,3} = \Omega_{4,5,6}$. Therefore

$$\lim_{\omega \to \omega_a} \mathbf{\Sigma^{-1}} = \mathbf{0}. \tag{94}$$

Thus, considering (94), the equation (93) reduces to

$$\mathbf{V}\mathbf{X}_p\left(j\omega_a\right) = \mathbf{0}. \tag{95}$$

Since matrix $\mathbf{V}$ is non-zero, it follows from the equation (95) that vector $\mathbf{X}_p$, given by (52), must be zero, yielding

$$\left[z_{P_1}(j\omega_a), z_{P_2}(j\omega_a), x_{P_3}(j\omega_a), x_{P_4}(j\omega_a), y_{P_5}(j\omega_a), y_{P_6}(j\omega_a)\right]^T = \mathbf{0} \tag{96}$$

regardless of the ω-harmonic force acting on the primary structure. Equation (96) also implies that complete damping occurs in the 6 coordinates of the points P_i defined by the vector $\mathbf{X}_p$. Considering the ideally rigid frame by which the absorber is fixed to the primary structure analogously to [35], the vibration would also be fully absorbed in the remaining coordinates and the harmonic excitation can be considered as completely absorbed at the collocated location.

In this paper, we however consider the entire primary structure (including the frame on which the actuators and springs are connected) as a general flexible structure described by modal model. Thus, the complete suppression of the vibration is realized fully only in those 6 directions. Considering the frame being stiff, considerable vibration reduction can be expected also in the remaining coordinates. Though, it is not guaranteed by the real design, the connection plates will be more or less similar as other elements of the primary structure. This issue will thoroughly be analysed in the simulation example.

Note also that the close-to ideal vibration suppression is synthesized only for the collocated deployment of the absorber. However, it is likely that the vibrations will be well suppressed also on some other locations on the primary structure. Thus, if the tuned absorber cannot be deployed at the target location to be silenced, the subsequent design

task can be formulated as optimizing the position on the primary to minimize the vibration at the target position. The effect of non-collocated deployment of the absorber will be analysed in the simulation example too. Another option for solving the non-collocated vibration absorption would be to respect the non-collocation in the absorber and DR feedback design. As shown in [39], [28], see also [30] and [31], for the one-dimensional problem, in such a case, the primary structure, or at least its part, need be included in the DR feedback synthesis. Considering the dimensionality of the problem and flexibility of the primary structure, such a solution would be fairly demanding for our design task. Therefore, we leave it for subsequent research.

7. Active absorber with delayed feedback

In Section 3, an ideal passive mechanical absorber (58) was proposed to absorb vibrations imposed by an ω-harmonic force acting at the primary structure. Further on, it was derived that all the natural frequencies need to satisfy $\Omega_{1,2,3} = \Omega_{4,5,6} = \omega$ and that the parameter absorber parameters I, m, R need to satisfy the constraint (65). For the ideal spring stiffness it implies

$$k_{ideal} = \frac{I\omega^2}{2R^2} = \frac{m\omega^2}{2}. \tag{97}$$

Note also that the ideal absorber (58) has no damping. These characteristics could hardly be achieved by a passive absorber. Besides, the frequency ω can vary in practice. In such a case, the absorber parameters need be re-tuned which is not easy to do for the passive absorber. Therefore, we apply an active delayed feedback to turn the physical absorber to the ideal absorber for the given excitation frequency.

Consider the active absorber with the configurations as in Figure 2 with the actuators imposing the forces u_i in the absorber links with the springs, given by

$$\mathbf{M}\ddot{\mathbf{X}}_a(t) + \tilde{\mathbf{C}}\dot{\mathbf{X}}_a(t) + \tilde{\mathbf{K}}\mathbf{X}_a(t) = \mathbf{L}\mathbf{u}(t), \tag{98}$$

where the mass matrix $\mathbf{M}$ has the same form as (53) and the stiffness and damping matrices are given by

$$\tilde{\mathbf{K}} = \begin{bmatrix} k_3+k_4 & 0 & 0 & 0 & 0 & (k_4-k_3)\,R \\ 0 & k_5+k_6 & 0 & (k_6-k_5)\,R & 0 & 0 \\ 0 & 0 & k_1+k_2 & 0 & (k_2-k_1)\,R & 0 \\ 0 & (k_6-k_5)\,R & 0 & (k_5+k_6)\,R^2 & 0 & 0 \\ 0 & 0 & (k_2-k_1)\,R & 0 & (k_1+k_2)\,R^2 & 0 \\ (k_4-k_3)\,R & 0 & 0 & 0 & 0 & (k_3+k_4)\,R^2 \end{bmatrix}, \tag{99}$$

$$\tilde{\mathbf{C}} = \begin{bmatrix} c_3+c_4 & 0 & 0 & 0 & 0 & (c_4-c_3)\,R \\ 0 & c_5+c_6 & 0 & (c_6-c_5)\,R & 0 & 0 \\ 0 & 0 & c_1+c_2 & 0 & (c_2-c_1)\,R & 0 \\ 0 & (c_6-c_5)\,R & 0 & (c_5+c_6)\,R^2 & 0 & 0 \\ 0 & 0 & (c_2-c_1)\,R & 0 & (c_1+c_2)\,R^2 & 0 \\ (c_4-c_3)\,R & 0 & 0 & 0 & 0 & (c_3+c_4)\,R^2 \end{bmatrix}, \tag{100}$$

where k_i and c_i are stiffness and damping coefficients of the i-th spring. Vector $\mathbf{u} = [u_1, u_2, u_3, u_4, u_5, u_6]^{\mathrm{T}}$ is the vector of actuator forces and

$$\mathbf{L} = \begin{bmatrix} 0 & 0 & 1 & 0 & -R & 0 \\ 0 & 0 & -1 & 0 & -R & 0 \\ 1 & 0 & 0 & 0 & 0 & -R \\ -1 & 0 & 0 & 0 & 0 & -R \\ 0 & 1 & 0 & -R & 0 & 0 \\ 0 & -1 & 0 & -R & 0 & 0 \end{bmatrix} \tag{101}$$

represents the projection of action forces to the absorber coordinates.

To tune the mechanical absorber parameters to an ideal unifrequency absorber, we consider the concept of a delayed resonator. Assume that each of the 6 absorber attachment springs has a sensor to measure the deflection l_i from the equilibrium position. Thus, analogously to the one-dimensional case (3), the delayed feedback actions have generally the form

$$u_i(t) = g_i l_i(t - \tau_i) \tag{102}$$

which in terms of the absorber coordinates can be transformed to

$$u_1(t) = g_1 \left(z_a(t - \tau_1) - R\varphi_y(t - \tau_1) - z_{p1}(t - \tau_1) \right), \tag{103}$$

$$u_2(t) = g_2 \left(z_a(t - \tau_2) + R\varphi_y(t - \tau_2) - z_{p2}(t - \tau_2) \right), \tag{104}$$

$$u_3(t) = g_3 \left(x_a(t - \tau_3) - R\varphi_z(t - \tau_3) - x_{p3}(t - \tau_3) \right), \tag{105}$$

$$u_4(t) = g_4 \left(x_a(t - \tau_4) + R\varphi_z(t - \tau_4) - x_{p4}(t - \tau_4) \right), \tag{106}$$

$$u_5(t) = g_5 \left(y_a(t - \tau_5) - R\varphi_x(t - \tau_5) - y_{p5}(t - \tau_5) \right), \tag{107}$$

$$u_6(t) = g_6 \left(y_a(t - \tau_6) + R\varphi_x(t - \tau_6) - y_{p6}(t - \tau_6) \right). \tag{108}$$

Similarly to the one-dimensional DR outlined in Subsection 2.1, the tuning of the gains g_i and delays τ_i is done by turning the physical link properties with k_i and c_i to the ideal link properties with k_{ideal} given by (97) and $c_{ideal} = 0$ by the active feedback (102). Analogously to (6), it leads to the following equality

$$g_i e^{-j\omega\tau_i} = jc_i\omega + k_i - k_{ideal} \tag{109}$$

from which we can express the gain g_i and the delay τ_i for an active spatial DR absorber. The first solution set is given by

$$g_i = -\sqrt{(k_i - k_{ideal})^2 + (\omega c_i)^2}, \tag{110}$$

$$\tau_i = \frac{1}{\omega} \left(\arctan \frac{\omega c_i}{k_{ideal} - k_i} + 2(\kappa - 1)\pi \right), \kappa = 1, 2, ... \tag{111}$$

and the other solution set is given by

$$g_i = \sqrt{(k_i - k_{ideal})^2 + (\omega c_i)^2}, \tag{112}$$

$$\tau_i = \frac{1}{\omega}\left(\arctan\frac{\omega c_i}{k_{ideal}-k_i} + (2\kappa-1)\pi\right), \kappa = 1,2,... \tag{113}$$

The dynamics equation of the resulting DR absorber is subsequently given by

$$\mathbf{M}\ddot{\mathbf{X}}_a + \tilde{\mathbf{C}}\dot{\mathbf{X}}_a + \mathbf{C}_p\dot{\mathbf{X}}_p + \tilde{\mathbf{K}}\mathbf{X}_a + \mathbf{K}_p\mathbf{X}_p - \sum_{i=1}^{6}\mathbf{G}_i\mathbf{X}_a(t-\tau_i) - \sum_{i=1}^{6}\mathbf{G}_{pi}\mathbf{X}_p(t-\tau_i) = \mathbf{0}. \tag{114}$$

Matrices $\mathbf{K}_p$, $\mathbf{C}_p$ have the same structure as in the case of ideal absorber (57) and along with the gain matrices $\mathbf{G}_i$ and $\mathbf{G}_{pi}$ derived from (102)-(103) they are given in Appendix A.

The state-space representation of the system with the active absorber attached has the following form

$$\dot{\mathbf{Z}} = \mathbf{A}\mathbf{Z} + \mathbf{B}_{\mathrm{F}}\mathrm{F} + \mathbf{B}_{\mathrm{P}}\left(\mathbf{S}_1\mathbf{X}_a + \mathbf{C}_1\dot{\mathbf{X}}_a - \sum_{i=1}^{6}\mathbf{H}_i\mathbf{X}_a(t-\tau_i)\right) + \mathbf{B}_{\mathrm{P}}\left(\mathbf{S}_2\mathbf{X}_p + \mathbf{C}_2\dot{\mathbf{X}}_p - \sum_{i=1}^{6}\mathbf{H}_{pi}\mathbf{X}_p(t-\tau_i)\right), \tag{115}$$

where

$$\mathbf{S}_1 = \begin{bmatrix} 0 & 0 & k_1 & 0 & -k_1R & 0 \\ 0 & 0 & k_2 & 0 & k_2R & 0 \\ k_3 & 0 & 0 & 0 & 0 & -k_3R \\ k_4 & 0 & 0 & 0 & 0 & k_4R \\ 0 & k_5 & 0 & -k_5R & 0 & 0 \\ 0 & k_6 & 0 & k_6R & 0 & 0 \end{bmatrix}, \mathbf{S}_2 = \begin{bmatrix} -k_1 & 0 & 0 & 0 & 0 & 0 \\ 0 & -k_2 & 0 & 0 & 0 & 0 \\ 0 & 0 & -k_3 & 0 & 0 & 0 \\ 0 & 0 & 0 & -k_4 & 0 & 0 \\ 0 & 0 & 0 & 0 & -k_5 & 0 \\ 0 & 0 & 0 & 0 & 0 & -k_6 \end{bmatrix}. \tag{116}$$

Substituting c_i instead of k_i into (116) gives the damping matrix $\mathbf{C}_1, \mathbf{C}_2$. The remaining matrices are the same as in the section 3. The gain matrices $\mathbf{H}_i$ and $\mathbf{H}_{pi}$ are composed in the same way as $\mathbf{G}_i$ and $\mathbf{G}_{pi}$ and can be found in Appendix A.

Substituting (82) into (114) and (115) and turning the equations to the Laplace form, the interconnection of the primary and the absorber reads as

$$\begin{bmatrix} s\mathbf{I} - \mathbf{A} - \mathbf{B}_{\mathrm{P}}\left(\mathbf{S}_2 + s\mathbf{C}_2 - \sum_{i=1}^{6}\mathbf{H}_{pi}e^{-s\tau_i}\right)\mathbf{C}_{abs} & -\mathbf{B}_{\mathrm{P}}\left(\mathbf{S}_1 + s\mathbf{C}_1 - \sum_{i=1}^{6}\mathbf{H}_i e^{-s\tau_i}\right) \\ \left(s\mathbf{C}_p + \mathbf{K}_p - \sum_{i=1}^{6}\mathbf{G}_{pi}e^{-s\tau_i}\right)\mathbf{C}_{abs} & s^2\mathbf{M} + s\tilde{\mathbf{C}} + \tilde{\mathbf{K}} - \sum_{i=1}^{6}\mathbf{G}_i e^{-s\tau_i} \end{bmatrix} \begin{bmatrix} \mathbf{Z}(s) \\ \mathbf{X}_a(s) \end{bmatrix} = \begin{bmatrix} \mathbf{B}_{\mathrm{F}}\mathrm{F}(s) \\ \mathbf{0} \end{bmatrix}. \tag{117}$$

Due to the introduction of the time delays, the interconnected system has infinitely many roots [40], which are given as the solutions of the characteristic equation

$$\det\left(\begin{bmatrix} s\mathbf{I} - \mathbf{A} - \mathbf{B}_{\mathrm{P}}\left(\mathbf{S}_2 + s\mathbf{C}_2 - \sum_{i=1}^{6}\mathbf{H}_{pi}e^{-s\tau_i}\right)\mathbf{C}_{abs} & -\mathbf{B}_{\mathrm{P}}\left(\mathbf{S}_1 + s\mathbf{C}_1 - \sum_{i=1}^{6}\mathbf{H}_i e^{-s\tau_i}\right) \\ \left(s\mathbf{C}_p + \mathbf{K}_p - \sum_{i=1}^{6}\mathbf{G}_{pi}e^{-s\tau_i}\right)\mathbf{C}_{abs} & s^2\mathbf{M} + s\tilde{\mathbf{C}} + \tilde{\mathbf{K}} - \sum_{i=1}^{6}\mathbf{G}_i e^{-s\tau_i} \end{bmatrix}\right) = 0. \tag{118}$$

For the interconnected system to be stable, all the infinitely many roots need to be located to the left of the stability boundary. As discussed thoroughly in [35], [34], the stability need be checked before the feedback implementation. The roots can be computed e.g. by TDS-CONTROL toolbox [41].

8. Simulation experiments

Simulation experiments were performed for both the collocated and the non-collocated deployment of the 3D-DR. The external excitation force acts at a different location (point F) from the absorber. The input is considered as one-dimensional in the form

$$\mathrm{F}(t) = \mathrm{F}_0 \cdot \sin(\omega t). \tag{119}$$

The force direction is given by chosen unity vector $\mathbf{e} = [e_x, e_y, e_z]^T$. For time simulation is chosen $\mathrm{F}_0 = 100$ N. The parameters listed in Table 2 were used in both the transfer function evaluation and the time simulation.

Table 2: Absorber parameters used for the simulation

Parameter		Value
Stiffness	k_1	11 187 N/m
	k_2	11 206 N/m
	k_3	11 152 N/m
	k_4	11 236 N/m
	k_5	11 050 N/m
	k_6	11 098 N/m
Damping	c_1	4.0 Ns/m
	c_2	5.5 Ns/m
	c_3	4.8 Ns/m
	c_4	3.7 Ns/m
	c_5	3.0 Ns/m
	c_6	4.4 Ns/m
Mass	m	100 kg
Size	R	500 mm
Spring free length	L	300 mm
Unity vector of excitation force	$\mathbf{e}$	$[0.5, 0.3, 0.81]^T$

8.1. Collocated absorption

In the collocated case we investigate the behaviour of the points P_i where the absorber is attached. Simulations were performed for two different absorber tuning: 15 rad/s and 20 rad/s. The absorber was tuned to these frequencies using the parameters found in Table 3. Note that when tuned to 20 rad/s, the required DR performance is significantly higher. This is because the absorber passive parameters (mass, spring stiffness) correspond to approximately 15 rad/s tuning.

Figure 4 shows the evaluation of the transfer function amplitude from the force excitation (119) to the directions given by $\mathbf{X}_p$. The black curves are amplitudes without

Table 3: Calculated gain and delay DR parameters for the tuning 15 rad/s and 20 rad/s

Gain	15 rad/s	20 rad/s	Delay	15 rad/s	20 rad/s
g_1	-87.0 N/m	-8 813 N/m	τ_1	0.0507 s	0.4539e-3 s
g_2	-93.5 N/m	-8 795 N/m	τ_2	0.0721 s	0.6254e-3 s
g_3	-121.6 N/m	-8 849 N/m	τ_3	0.0422 s	0.5425e-3 s
g_4	-57.2 N/m	-8 764 N/m	τ_4	0.0882 s	0.4222e-3 s
g_5	-205.0 N/m	-8 950 N/m	τ_5	0.0148 s	0.3352e-3 s
g_6	-165.7 N/m	-8 902 N/m	τ_6	0.0273 s	0.4943e-3 s

absorber, the red curves are with absorber tuned to 20 rad/s. The graphs in the right column show the detail in the absorber tuning zone. Complete suppression occurs in all directions $\mathbf{X}_p$, which is consistent with the derivation in Section 6.

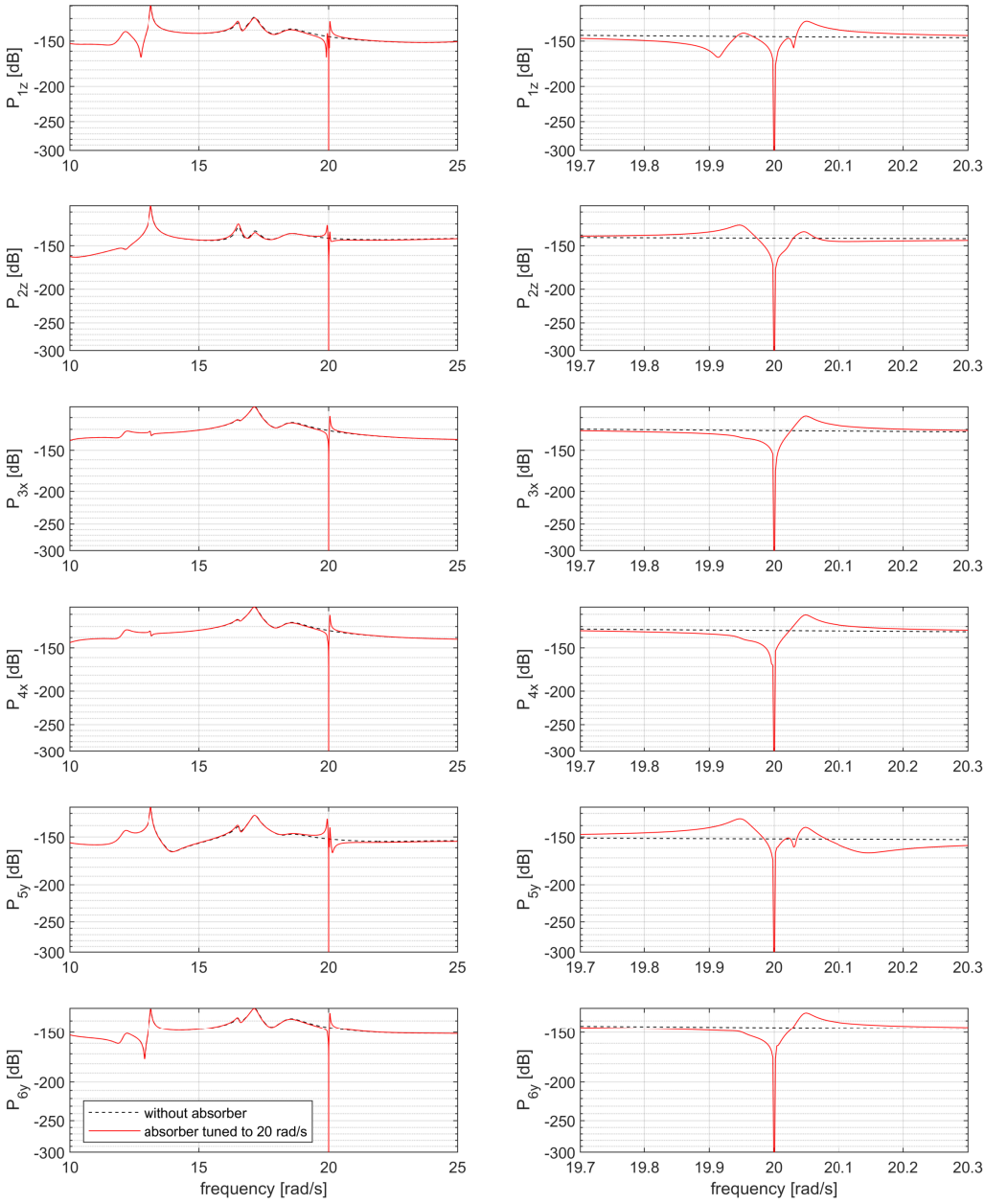


Figure 4: Evaluation of the transfer function amplitude from the force excitation (119) to the directions given by $\mathbf{X}_p$ (collocated case), absorber tuned to ω_a=20 rad/s, the right figures zoom in around ω_a

Figure 5 and Figure 6 show the evaluation of the transfer function amplitude from the force excitation (119) to the vibrations of connection point P_1. The black curve represents the situation without absorber, the blue curve in Figure 5 and the red curve

in Figure 6 are achieved with the absorber tuned to 15 rad/s and 20 rad/s, respectively. The graphs in the right column show the detail in the absorber tuning zone. According to the previously derived relations, complete vibration suppression is achieved only in the z-direction, which is the only P_1 coordinate that appears in $\mathbf{X}_p$. Both figures show that some amount of vibration suppression occurs in other directions as well, but complete suppression is achieved in the z-direction only.

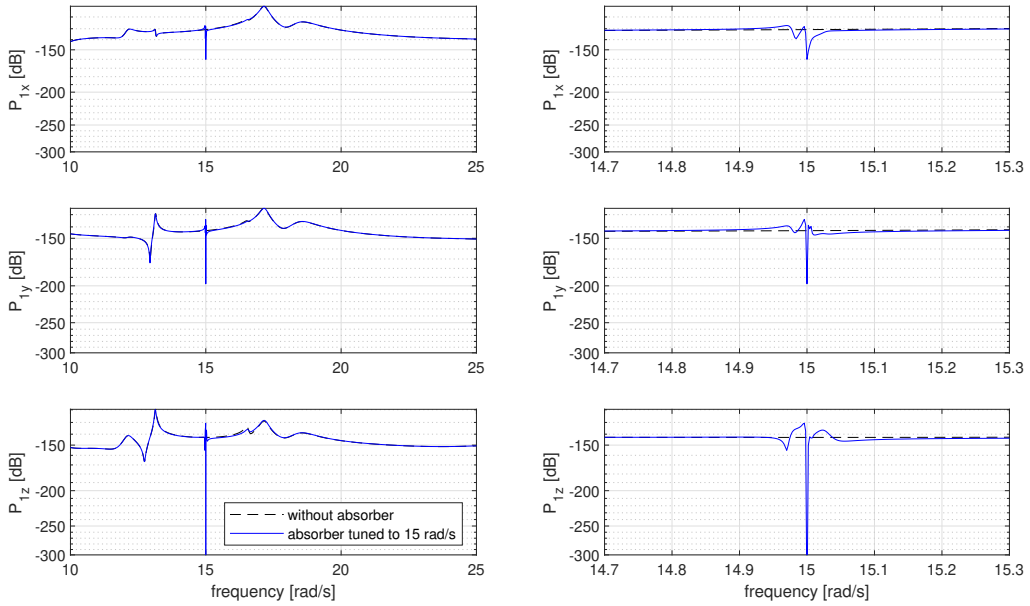


Figure 5: Evaluation of the transfer function amplitude from the force excitation (119) to the vibrations of connection point P_1, absorber tuned to ω_a=15 rad/s, the right figures zoom in around ω_a

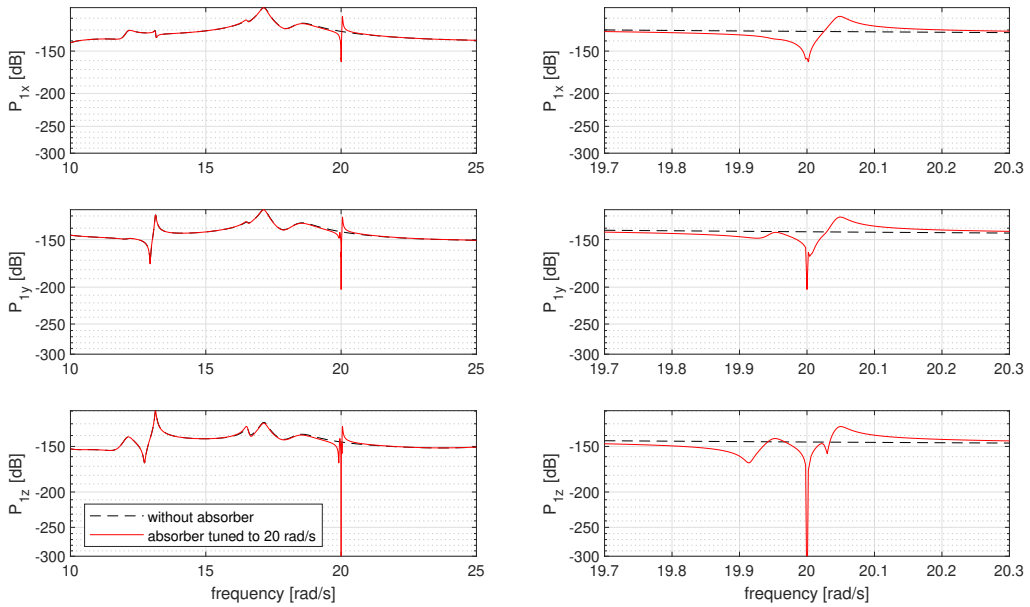


Figure 6: Evaluation of the transfer function amplitude from the force excitation (119) to the vibrations of connection point P_1, absorber tuned to ω_a=20 rad/s, the right figures zoom in around ω_a

The calculated values of the transfer function amplitude at all points P_i are given in Table 4 for both excitation frequencies 15 rad/s and 20 rad/s. The results are compared to the values without absorber. The coordinates from the $\mathbf{X}_p$ vector are highlighted in bold. Complete suppression occurs for each point P_i in the direction of the attached spring. This result is consistent with the derived assumption (96).

Table 4: Evaluation of the amplitude of the transfer function from the force excitation (119) to the vibrations of connection points P_i for the absorber tuned to the frequency matching the excitation frequency of 15 rad/s and 20 rad/s

Point	$\|G(j\omega)\|$ without absorber, $\omega =$ 15 rad/s	$\|G(j\omega)\|$ with absorber, $\omega = \omega_a =$ 15 rad/s	$\|G(j\omega)\|$ without absorber, $\omega =$ 20 rad/s	$\|G(j\omega)\|$ with absorber, $\omega = \omega_a =$ 20 rad/s
P_{1x}	2.8964e-07	9.9154e-09	2.7389e-07	1.3296e-08
P_{1y}	6.8970e-08	1.3216e-10	7.0227e-08	7.2702e-11
$\boldsymbol{P_{1z}}$	**7.1675e-08**	**1.9297e-22**	**5.0999e-08**	**5.6416e-23**
P_{2x}	2.1585e-07	9.9154e-09	2.1348e-07	1.3296e-08
P_{2y}	4.1249e-08	1.3216e-10	4.3583e-08	7.2702e-11
$\boldsymbol{P_{2z}}$	**5.8767e-08**	**1.4696e-22**	**7.2581e-08**	**6.4520e-23**
$\boldsymbol{P_{3x}}$	**2.9083e-07**	**1.6519e-22**	**2.7829e-07**	**8.2003e-23**
P_{3y}	9.7679e-09	4.0231e-10	8.0173e-09	2.8754e-10
P_{3z}	4.1539e-08	1.5442e-08	1.6150e-08	2.4667e-08
$\boldsymbol{P_{4x}}$	**2.1467e-07**	**1.5519e-22**	**2.0908e-07**	**6.7581e-23**
P_{4y}	3.7152e-08	4.0231e-10	3.4497e-08	2.8754e-10
P_{4z}	1.0883e-07	1.5442e-08	1.1110e-07	2.4667e-08
P_{5x}	1.6879e-07	1.6513e-08	1.7308e-07	2.1090e-08
$\boldsymbol{P_{5y}}$	**1.6423e-08**	**5.5215e-23**	**2.5874e-08**	**1.3957e-22**
P_{5z}	1.5130e-07	3.4166e-08	1.8279e-07	5.4399e-08
P_{6x}	3.3670e-07	1.6513e-08	3.1430e-07	2.1090e-08
$\boldsymbol{P_{6y}}$	**4.3422e-08**	**2.0392e-23**	**5.2160e-08**	**6.9926e-23**
P_{6z}	4.4830e-08	3.4166e-08	6.1376e-08	5.4399e-08

8.2. Absorption at non-collocated locations

Now we focus on the non-collocated absorption, i.e., on the points of the system where the absorber is not attached. We consider that the point F, where the excitation force is applied, the absorber position and the point of interest N are three different locations. In contrast to the collocated case, we now have no exact relation that guarantees vibration suppression. Of the 63 points defined on the primary mass, 39 were considered for the placement of the absorber. The schema in Figure 3 shows two such points, labeled S_i and S_j. The specific position of the points on the structure is shown in Figure 7. The amplitude of the transfer function from the force excitation (119) to the vibrations of point N was evaluated for placing the absorber at each of these points. The spatial harmonic excitation force was defined by amplitude 100 N, frequency 15 rad/s and direction unity vector $\mathbf{e} = [0.5, 0.3, 0.81]^T$. Two criteria were considered. The first was the norm of the amplitude in the direction of all three coordinate axes x, y, z. The second criterion was the maximum of these three values. The results are presented in Figure 8). It is shown that for both criteria, point no. 57 is the most suitable for the location of the absorber. Note that partial vibration suppression occurs when placed at either point. The values of the criteria are always lower than the values without the absorber, which are shown by the solid and dashed lines.

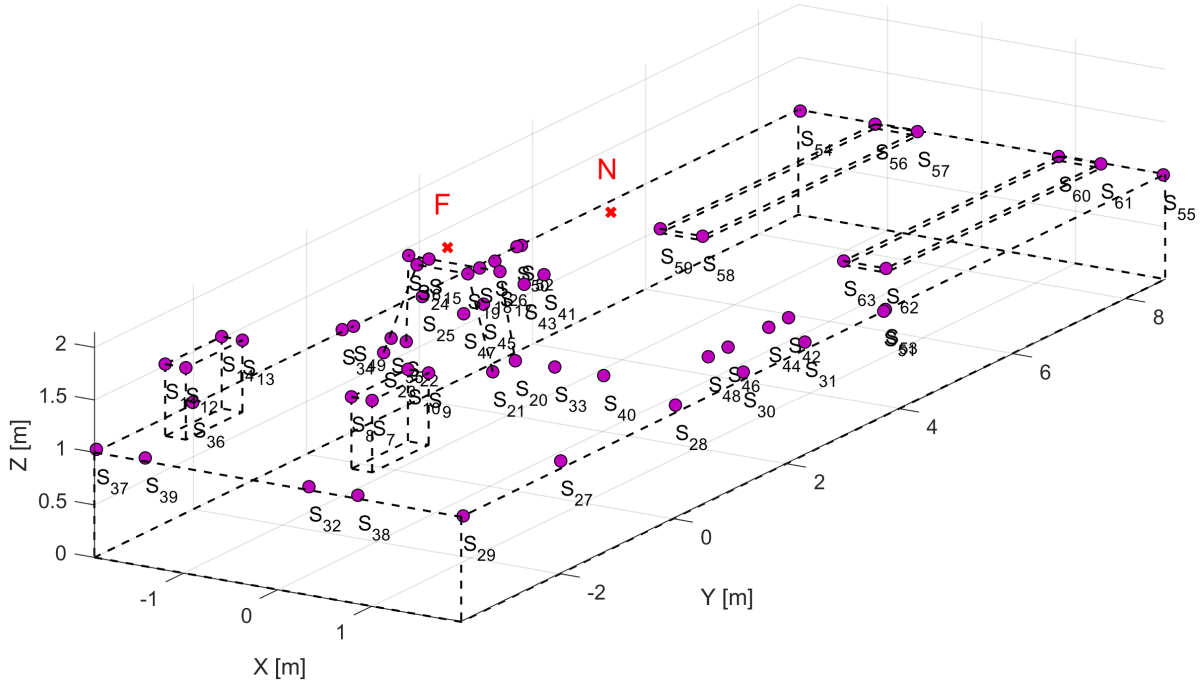


Figure 7: Considered absorber locations

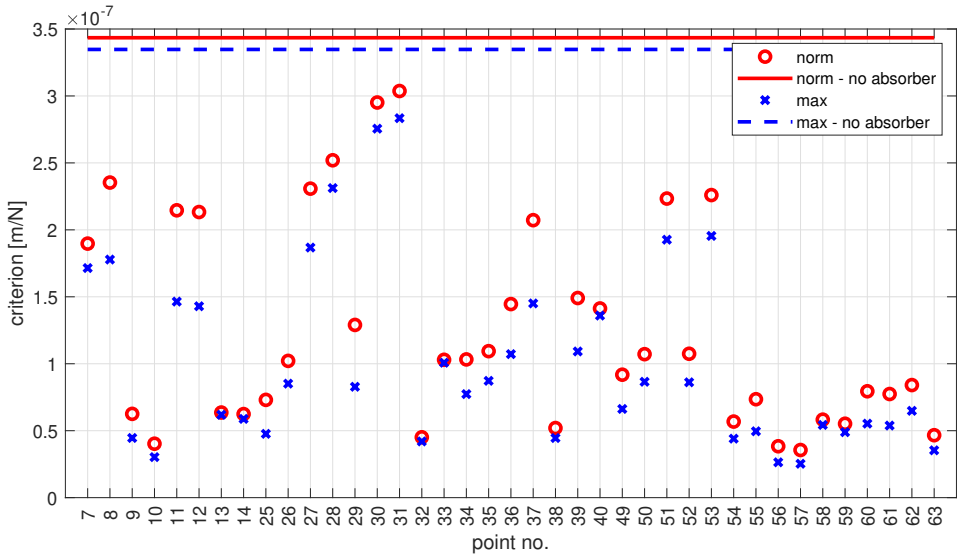


Figure 8: Comparison of normalized and maximum criterion values for different absorber locations

The time domain response is shown in Figure 9. For sufficient excitation, the amplitude of the excitation force was increased to 1000 N. It is seen that there is a progressive suppression of vibration at the non-collocated point. This suppression is very slow because the mass of the absorber is small compared to the primary mass. For the next simulation,

the mass of the absorber was increased to 1000 kg. The stiffness and damping coefficients were also multiplied by a factor of 10 to maintain the tuning. The time response is shown in Figure 10. The active absorber was started at time $t = 50$ s . The response without absorber is shown in Figure 11. From the comparison of the two waveforms, it is clear that by using the active absorber, the vibration amplitude was reduced by a factor of 10. This is consistent with the results of the analysis in Figure 8.

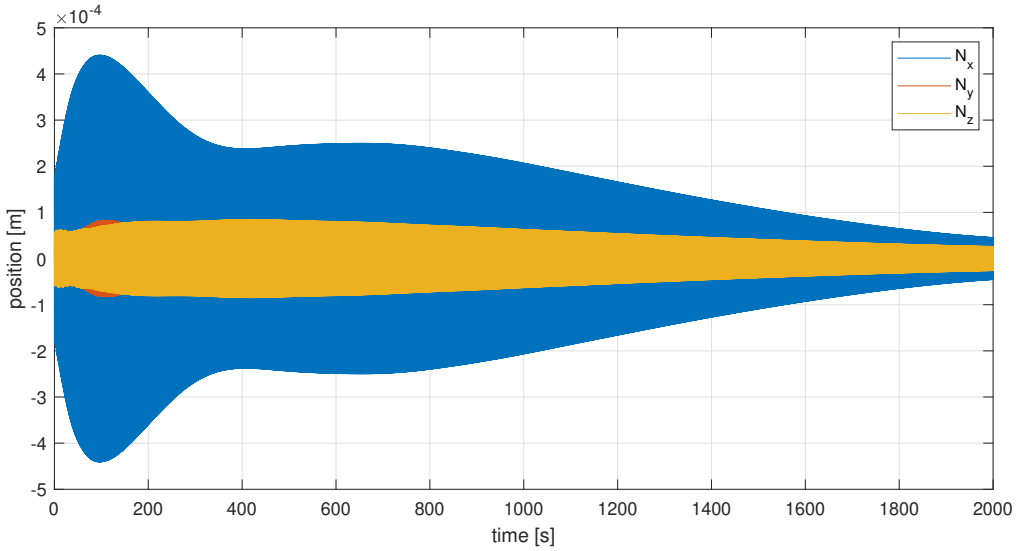


Figure 9: Response at the non-collocated point N, absorber 100 kg in S_{57}

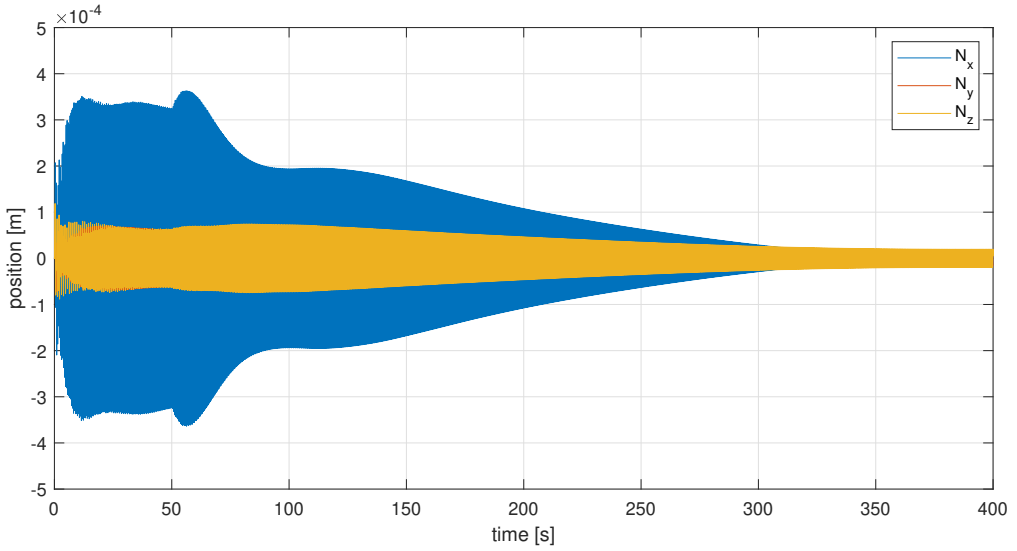


Figure 10: Response at the non-collocated point N, absorber 1000 kg in S_{57} was switched on at $t = 50$ s

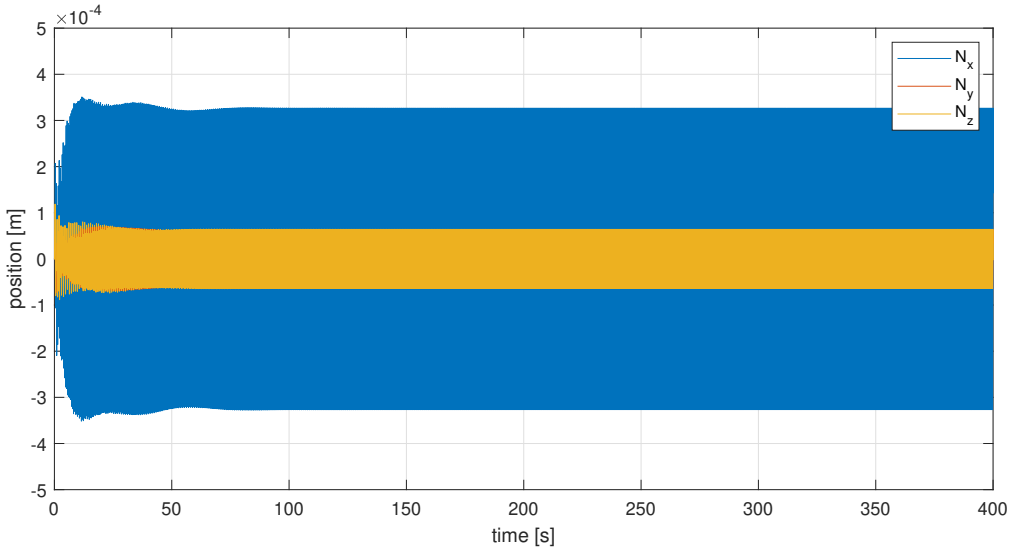


Figure 11: Response at the point N without absorber

9. Conclusion

The presented work dealt with a significant extension of the concept of active absorbers with multiple degrees of freedom and a single multiple eigenfrequency (unifrequency property/dynamic isotropy) for absorbing vibrations in spatial flexible systems with many degrees of freedom. A compact spatial absorber with six degrees of freedom was designed, which is able to achieve unifrequency only mechanically for ideal stiffness and mass parameters. Despite this theoretical passive (only mechanically achievable) dynamic isotropy, active correction by actuators is always necessary. This is mainly due to spring stiffness deviations, geometry errors and non-zero mechanical damping. Consequently the actuators are added in parallel with the springs and a spatial generalization of the delayed resonator [19, 33] concept (3D-DR) is used. The relative motion position sensors were considered for the feedback used in the DR.

The absorber was attached to a three-dimensional flexible frame with many degrees of freedom transformed to a reduced order model in modal coordinates with residuum. The entire system with the absorber was modeled and it was deduced that for any external harmonic excitation force there is complete vibration suppression in one defined direction for each of the six points of attachment of the absorber to the primary flexible system. It was also shown that in the other directions of these six attachment points there will also be vibration suppression, but not total. After investigating the properties of collocated vibration absorption of the flexible spatial system, the possibilities of non-collocated vibration reduction were studied. This possibility is technically important, because very often it is not possible to place the absorber in the same place where we need to suppress vibrations. The influence of the position of the absorber on the flexible system and its parameters was investigated. A solution to the non-collocated problem was found causing an order-of-magnitude reduction in the oscillation amplitude of the investigated location of the primary flexible system.

The possible use of a unifrequency spatial absorber for vibration absorption of complex spatial flexible systems was demonstrated, as well as a potential for optimizing this task for a specific application in the technical practice. The absorber has considerable potential for use in improving the dynamic behaviour of robots, complex rotor systems and other mechanical systems suffering from unwanted fully spatial vibrations.

Acknowledgment

The presented research was supported by the Czech Science Foundation under the project 21-00871S "Active non-collocated vibration absorption for robots and mechanical structures", and by the Europen Union under the project "Robotics and advanced industrial production", reg. no. CZ.02.01.01/00/22_008/0004590. Wim Michiels was supported by the project project C14/22/092 of the Internal Funds KU Leuven and the project G092721N of the Research Foundation-Flanders (FWO - Vlaanderen).

References

[1] M. Kasprowiak, A. Parus, M. Hoffmann, Vibration suppression with use of input shaping control in machining, Sensors 22 (6) (2022).

[2] V. Nguyen, J. Johnson, S. Melkote, Active vibration suppression in robotic milling using optimal control, International Journal of Machine Tools and Manufacture 152 (2020) 103541.

[3] P. Beneš, M. Valášek, Z. Šika, J. Zavřel, J. Pelikán, Shavo control: the combination of the adjusted command shaping and feedback control for vibration suppression, Acta Mechanica 230 (5) (2019) 1891–1905.

[4] A. Genno, W. Wang, An adaptive neuro-fuzzy controller for vibration suppression of flexible structuress, IEEE/ASME Transactions on Mechatronics 29 (2) (2024) 1342–1351.

[5] S. N. Mahmoodi, M. Ahmadian, D. J. Inman, Adaptive modified positive position feedback for active vibration control of structures, Journal of Intelligent Material Systems and Structures 21 (6) (2010) 571–580.

[6] U. H. Diala, Y. Zhu, Z.-Q. Lang, Analysis of the energy dissipation characteristics of a nonlinear vehicle suspension system, in: 2022 UKACC 13th International Conference on Control (CONTROL), 2022, pp. 177–182.

[7] R. Rana, T. Soong, Parametric study and simplified design of tuned mass dampers, Engineering Structures 20 (3) (1998) 193–204.

[8] W. Ma, Y. Yang, J. Yu, General routine of suppressing single vibration mode by multi-dof tuned mass damper: application of three-dof, Mechanical Systems and Signal Processing 121 (2019) 77–96.

[9] F. Chen, H. Zhao, D. Li, L. Chen, C. Tan, H. Ding, Contact force control and vibration suppression in robotic polishing with a smart end effector, Robotics and Computer-Integrated Manufacturing 57 (2019) 391–403.

[10] H. Zuo, K. Bi, H. Hao, Using multiple tuned mass dampers to control offshore wind turbine vibrations under multiple hazards, Engineering Structures 141 (2017) 303–315.

[11] T. Aksoy, G. O. Ozgen, B. Acar, Design of a tuned vibration absorber for a slender hollow cylindrical structure, Mechanics Based Design of Structures and Machines 48 (5) (2020) 615–648.
[12] P. Gao, H. Li, H. Liu, C. Xiang, An innovative torsional vibration absorber of vehicle powertrain system: Prototype design, performance test, and control experiment, Mechanics Based Design of Structures and Machines 51 (6) (2023) 3434–3466.
[13] A. Preumont, Vibration control of active structures: an introduction, Vol. 246, Springer, 2018.
[14] N. Olgac, N. Jalili, Modal analysis of flexible beams with delayed resonator vibration absorber: theory and experiments, Journal of Sound and Vibration 218 (2) (1998) 307–331.
[15] N. Jalili, N. Olgac, Multiple delayed resonator vibration absorbers for multi-degree-of-freedom mechanical structures, Journal of Sound and Vibration 223 (4) (1999) 567–585.
[16] M. Hosek, N. Olgac, A single-step automatic tuning algorithm for the delayed resonator vibration absorber, IEEE/ASME Transactions on Mechatronics 7 (2) (2002) 245–255.
[17] N. Olgac, B. Holm-Hansen, A novel active vibration absorption technique: delayed resonator, Journal of Sound and Vibration 176 (1) (1994) 93–104.
[18] D. Filipović, N. Olgac, Delayed resonator with speed feedback–design and performance analysis, Mechatronics 12 (3) (2002) 393–413.
[19] N. Olgac, H. Elmali, M. Hosek, M. Renzulli, Active vibration control of distributed systems using delayed resonator with acceleration feedback, Journal of Dynamic Systems, Measurement, and Control 119 (3) (1997) 380–389.
[20] T. Vyhlídal, N. Olgac, V. Kučera, Delayed resonator with acceleration feedback–complete stability analysis by spectral methods and vibration absorber design, Journal of Sound and Vibration 333 (25) (2014) 6781–6795.
[21] D. Pilbauer, T. Vyhlidal, N. Olgac, Delayed resonator with distributed delay in acceleration feedback - design and experimental verification, IEEE/ASME Transactions on Mechatronics 21 (4) (2016) 2120–2131.
[22] V. Kučera, D. Pilbauer, T. Vyhlídal, N. Olgac, Extended delayed resonators–design and experimental verification, Mechatronics 41 (2017) 29–44.
[23] D. Pilbauer, T. Vyhlídal, W. Michiels, Spectral design of output feedback controllers for systems pre-compensated by input shapers, in: Proceedings of the 12th IFAC Workshop on Time-Delay Systems, 2015, pp. 1–6.
[24] M. Kuře, T. Vyhlídal, W. Michiels, I. Boussaada, Spectral design of robust delayed resonator by double-root assignment, IFAC-PapersOnLine 51 (14) (2018) 72–77.
[25] T. Vyhlídal, D. Pilbauer, B. Alikoç, W. Michiels, Analysis and design aspects of delayed resonator absorber with position, velocity or acceleration feedback, Journal of Sound and Vibration 459 (2019) 114831.
[26] M. Valášek, N. Olgac, Z. Neusser, Real-time tunable single-degree of freedom, multiple-frequency vibration absorber, Mechanical Systems and Signal Processing 133 (2019) 106244.
[27] R. Jenkins, N. Olgac, Real-time tuning of delayed resonator-based absorbers for spectral and spatial variations, Journal of Vibration and Acoustics 141 (2) (2019).

[28] N. Olgac, R. Jenkins, Actively tuned noncollocated vibration absorption: An unexplored venue in vibration science and a benchmark problem, IEEE Transactions on Control Systems Technology 29 (1) (2021) 294–304.
[29] D. Filipović, D. Schröder, Control of vibrations in multi-mass systems with locally controlled absorbers, Automatica 37 (2) (2001) 213–220.
[30] H. Silm, M. Kuře, J. Bušek, W. Michiels, T. Vyhlídal, Spectral design and experimental validation of noncollocated vibration suppression by a delayed resonator and time-delay controller, IEEE Transactions on Control Systems Technology 32 (1) (2024) 73–85.
[31] A. Saldanha, W. Michiels, M. Kuře, J. Bušek, T. Vyhlídal, Stability optimization of time-delay systems with zero-location constraints applied to non-collocated vibration suppression, Mechanical Systems and Signal Processing 208 (2024) 110886.
[32] K. Kraus, Z. Šika, P. Beneš, J. Krivošej, T. Vyhlídal, Mechatronic robot arm with active vibration absorbers, Journal of Vibration and Control 26 (13-14) (2020) 1145–1156.
[33] Z. Šika, T. Vyhlídal, Z. Neusser, Two-dimensional delayed resonator for entire vibration absorption, Journal of Sound and Vibration 500 (2021) 116010.
[34] T. Vyhlídal, W. Michiels, Z. Neusser, J. Bušek, Z. Šika, Analysis and optimized design of an actively controlled two-dimensional delayed resonator, Mechanical Systems and Signal Processing 178 (2022) 109195.
[35] Z. Šika, J. Krivošej, T. Vyhlídal, Three dimensional delayed resonator of stewart platform type for entire absorption of fully spatial vibration, Journal of Sound and Vibration 571 (2024) 118154.
[36] Z. Šika, J. Zavřel, M. Valášek, Residual modes for structure reduction and efficient coupling of substructures, Bulletin of Applied Mechanics 5 (19) (2009) 54–59.
[37] G. Obinata, B. Anderson, Model reduction for control system design, Applied Mechanics Reviews 54 (5) (2001) B81–B82.
[38] V. Stejskal, M. Valášek, Kinematics and Dynamics of Machinery, Marcel Dekker, New York, 1996.
[39] N. Olgac, R. Jenkins, Actively tuned noncollocated vibration absorption: An unexplored venue in vibration science and a benchmark problem, IEEE Transactions on Control Systems Technology 29 (1) (2020) 294–304.
[40] J. K. Hale, Functional differential equations, in: Analytic Theory of Differential Equations, Springer, 1971, pp. 9–22.
[41] P. Appeltans, H. Silm, W. Michiels, Tds-control: A matlab package for the analysis and controller-design of time-delay systems, IFAC-PapersOnLine 55 (16) (2022) 272–277.

Appendix A.

Stiffness, damping and gain matrices used in (114)

$$\mathbf{K}_p = \begin{bmatrix} 0 & 0 & -k_3 & -k_4 & 0 & 0 \\ 0 & 0 & 0 & 0 & -k_5 & -k_6 \\ -k_1 & -k_2 & 0 & 0 & 0 & 0 \\ 0 & 0 & 0 & 0 & k_5 R & -k_6 R \\ k_1 R & -k_2 R & 0 & 0 & 0 & 0 \\ 0 & 0 & k_3 R & -k_4 R & 0 & 0 \end{bmatrix}. \tag{A.1}$$

$$\mathbf{C}_p = \begin{bmatrix} 0 & 0 & -c_3 & -c_4 & 0 & 0 \\ 0 & 0 & 0 & 0 & -c_5 & -c_6 \\ -c_1 & -c_2 & 0 & 0 & 0 & 0 \\ 0 & 0 & 0 & 0 & c_5 R & -c_6 R \\ c_1 R & -c_2 R & 0 & 0 & 0 & 0 \\ 0 & 0 & c_3 R & -c_4 R & 0 & 0 \end{bmatrix}. \tag{A.2}$$

$$\mathbf{G}_1 = \begin{bmatrix} 0 & 0 & 0 & 0 & 0 & 0 \\ 0 & 0 & 0 & 0 & 0 & 0 \\ 0 & 0 & g_1 & 0 & -g_1 R & 0 \\ 0 & 0 & 0 & 0 & 0 & 0 \\ 0 & 0 & -g_1 R & 0 & g_1 R^2 & 0 \\ 0 & 0 & 0 & 0 & 0 & 0 \end{bmatrix}, \mathbf{G}_{p1} = \begin{bmatrix} 0 & 0 & 0 & 0 & 0 & 0 \\ 0 & 0 & 0 & 0 & 0 & 0 \\ -g_1 & 0 & 0 & 0 & 0 & 0 \\ 0 & 0 & 0 & 0 & 0 & 0 \\ g_1 R & 0 & 0 & 0 & 0 & 0 \\ 0 & 0 & 0 & 0 & 0 & 0 \end{bmatrix} \tag{A.3}$$

$$\mathbf{G}_2 = \begin{bmatrix} 0 & 0 & 0 & 0 & 0 & 0 \\ 0 & 0 & 0 & 0 & 0 & 0 \\ 0 & 0 & g_2 & 0 & g_2 R & 0 \\ 0 & 0 & 0 & 0 & 0 & 0 \\ 0 & 0 & g_2 R & 0 & g_2 R^2 & 0 \\ 0 & 0 & 0 & 0 & 0 & 0 \end{bmatrix}, \mathbf{G}_{p2} = \begin{bmatrix} 0 & 0 & 0 & 0 & 0 & 0 \\ 0 & 0 & 0 & 0 & 0 & 0 \\ 0 & -g_2 & 0 & 0 & 0 & 0 \\ 0 & 0 & 0 & 0 & 0 & 0 \\ 0 & -g_2 R & 0 & 0 & 0 & 0 \\ 0 & 0 & 0 & 0 & 0 & 0 \end{bmatrix} \tag{A.4}$$

$$\mathbf{G}_3 = \begin{bmatrix} g_3 & 0 & 0 & 0 & 0 & -g_3 R \\ 0 & 0 & 0 & 0 & 0 & 0 \\ 0 & 0 & 0 & 0 & 0 & 0 \\ 0 & 0 & 0 & 0 & 0 & 0 \\ 0 & 0 & 0 & 0 & 0 & 0 \\ -g_3 R & 0 & 0 & 0 & 0 & g_3 R^2 \end{bmatrix}, \mathbf{G}_{p3} = \begin{bmatrix} 0 & 0 & -g_3 & 0 & 0 & 0 \\ 0 & 0 & 0 & 0 & 0 & 0 \\ 0 & 0 & 0 & 0 & 0 & 0 \\ 0 & 0 & 0 & 0 & 0 & 0 \\ 0 & 0 & 0 & 0 & 0 & 0 \\ 0 & 0 & g_3 R & 0 & 0 & 0 \end{bmatrix} \tag{A.5}$$

$$\mathbf{G}_4 = \begin{bmatrix} g_4 & 0 & 0 & 0 & 0 & g_4 R \\ 0 & 0 & 0 & 0 & 0 & 0 \\ 0 & 0 & 0 & 0 & 0 & 0 \\ 0 & 0 & 0 & 0 & 0 & 0 \\ 0 & 0 & 0 & 0 & 0 & 0 \\ g_4 R & 0 & 0 & 0 & 0 & g_4 R^2 \end{bmatrix}, \mathbf{G}_{p4} = \begin{bmatrix} 0 & 0 & 0 & -g_4 & 0 & 0 \\ 0 & 0 & 0 & 0 & 0 & 0 \\ 0 & 0 & 0 & 0 & 0 & 0 \\ 0 & 0 & 0 & 0 & 0 & 0 \\ 0 & 0 & 0 & 0 & 0 & 0 \\ 0 & 0 & 0 & -g_4 R & 0 & 0 \end{bmatrix} \tag{A.6}$$

$$\mathbf{G}_5 = \begin{bmatrix} 0 & 0 & 0 & 0 & 0 & 0 \\ 0 & g_5 & 0 & -g_5R & 0 & 0 \\ 0 & 0 & 0 & 0 & 0 & 0 \\ 0 & -g_5R & 0 & g_5R^2 & 0 & 0 \\ 0 & 0 & 0 & 0 & 0 & 0 \\ 0 & 0 & 0 & 0 & 0 & 0 \end{bmatrix}, \mathbf{G}_{p5} = \begin{bmatrix} 0 & 0 & 0 & 0 & 0 & 0 \\ 0 & 0 & 0 & 0 & -g_5 & 0 \\ 0 & 0 & 0 & 0 & 0 & 0 \\ 0 & 0 & 0 & 0 & g_5R & 0 \\ 0 & 0 & 0 & 0 & 0 & 0 \\ 0 & 0 & 0 & 0 & 0 & 0 \end{bmatrix} \tag{A.7}$$

$$\mathbf{G}_6 = \begin{bmatrix} 0 & 0 & 0 & 0 & 0 & 0 \\ 0 & g_6 & 0 & g_6R & 0 & 0 \\ 0 & 0 & 0 & 0 & 0 & 0 \\ 0 & g_6R & 0 & g_6R^2 & 0 & 0 \\ 0 & 0 & 0 & 0 & 0 & 0 \\ 0 & 0 & 0 & 0 & 0 & 0 \end{bmatrix}, \mathbf{G}_{p6} = \begin{bmatrix} 0 & 0 & 0 & 0 & 0 & 0 \\ 0 & 0 & 0 & 0 & 0 & -g_6 \\ 0 & 0 & 0 & 0 & 0 & 0 \\ 0 & 0 & 0 & 0 & 0 & -g_6R \\ 0 & 0 & 0 & 0 & 0 & 0 \\ 0 & 0 & 0 & 0 & 0 & 0 \end{bmatrix} \tag{A.8}$$

$$\mathbf{H}_1 = \begin{bmatrix} 0 & 0 & g_1 & 0 & -g_1R & 0 \\ 0 & 0 & 0 & 0 & 0 & 0 \\ 0 & 0 & 0 & 0 & 0 & 0 \\ 0 & 0 & 0 & 0 & 0 & 0 \\ 0 & 0 & 0 & 0 & 0 & 0 \\ 0 & 0 & 0 & 0 & 0 & 0 \end{bmatrix}, \mathbf{H}_{p1} = \begin{bmatrix} -g_1 & 0 & 0 & 0 & 0 & 0 \\ 0 & 0 & 0 & 0 & 0 & 0 \\ 0 & 0 & 0 & 0 & 0 & 0 \\ 0 & 0 & 0 & 0 & 0 & 0 \\ 0 & 0 & 0 & 0 & 0 & 0 \\ 0 & 0 & 0 & 0 & 0 & 0 \end{bmatrix} \tag{A.9}$$

$$\mathbf{H}_2 = \begin{bmatrix} 0 & 0 & 0 & 0 & 0 & 0 \\ 0 & 0 & g_2 & 0 & g_2R & 0 \\ 0 & 0 & 0 & 0 & 0 & 0 \\ 0 & 0 & 0 & 0 & 0 & 0 \\ 0 & 0 & 0 & 0 & 0 & 0 \\ 0 & 0 & 0 & 0 & 0 & 0 \end{bmatrix}, \mathbf{H}_{p2} = \begin{bmatrix} 0 & 0 & 0 & 0 & 0 & 0 \\ 0 & -g_2 & 0 & 0 & 0 & 0 \\ 0 & 0 & 0 & 0 & 0 & 0 \\ 0 & 0 & 0 & 0 & 0 & 0 \\ 0 & 0 & 0 & 0 & 0 & 0 \\ 0 & 0 & 0 & 0 & 0 & 0 \end{bmatrix} \tag{A.10}$$

$$\mathbf{H}_3 = \begin{bmatrix} 0 & 0 & 0 & 0 & 0 & 0 \\ 0 & 0 & 0 & 0 & 0 & 0 \\ g_3 & 0 & 0 & 0 & 0 & -g_3R \\ 0 & 0 & 0 & 0 & 0 & 0 \\ 0 & 0 & 0 & 0 & 0 & 0 \\ 0 & 0 & 0 & 0 & 0 & 0 \end{bmatrix}, \mathbf{H}_{p3} = \begin{bmatrix} 0 & 0 & 0 & 0 & 0 & 0 \\ 0 & 0 & 0 & 0 & 0 & 0 \\ 0 & 0 & -g_3 & 0 & 0 & 0 \\ 0 & 0 & 0 & 0 & 0 & 0 \\ 0 & 0 & 0 & 0 & 0 & 0 \\ 0 & 0 & 0 & 0 & 0 & 0 \end{bmatrix} \tag{A.11}$$

$$\mathbf{H}_4 = \begin{bmatrix} 0 & 0 & 0 & 0 & 0 & 0 \\ 0 & 0 & 0 & 0 & 0 & 0 \\ 0 & 0 & 0 & 0 & 0 & 0 \\ g_4 & 0 & 0 & 0 & 0 & g_4R \\ 0 & 0 & 0 & 0 & 0 & 0 \\ 0 & 0 & 0 & 0 & 0 & 0 \end{bmatrix}, \mathbf{H}_{p4} = \begin{bmatrix} 0 & 0 & 0 & 0 & 0 & 0 \\ 0 & 0 & 0 & 0 & 0 & 0 \\ 0 & 0 & 0 & 0 & 0 & 0 \\ 0 & 0 & 0 & -g_4 & 0 & 0 \\ 0 & 0 & 0 & 0 & 0 & 0 \\ 0 & 0 & 0 & 0 & 0 & 0 \end{bmatrix} \tag{A.12}$$

$$\mathbf{H}_5 = \begin{bmatrix} 0 & 0 & 0 & 0 & 0 & 0 \\ 0 & 0 & 0 & 0 & 0 & 0 \\ 0 & 0 & 0 & 0 & 0 & 0 \\ 0 & 0 & 0 & 0 & 0 & 0 \\ 0 & g_5 & 0 & -g_5R & 0 & 0 \\ 0 & 0 & 0 & 0 & 0 & 0 \end{bmatrix}, \mathbf{H}_{p5} = \begin{bmatrix} 0 & 0 & 0 & 0 & 0 & 0 \\ 0 & 0 & 0 & 0 & 0 & 0 \\ 0 & 0 & 0 & 0 & 0 & 0 \\ 0 & 0 & 0 & 0 & 0 & 0 \\ 0 & 0 & 0 & 0 & -g_5 & 0 \\ 0 & 0 & 0 & 0 & 0 & 0 \end{bmatrix} \tag{A.13}$$

$$\mathbf{H}_6 = \begin{bmatrix} 0 & 0 & 0 & 0 & 0 & 0 \\ 0 & 0 & 0 & 0 & 0 & 0 \\ 0 & 0 & 0 & 0 & 0 & 0 \\ 0 & 0 & 0 & 0 & 0 & 0 \\ 0 & 0 & 0 & 0 & 0 & 0 \\ 0 & g_6 & 0 & g_6 R & 0 & 0 \end{bmatrix}, \mathbf{H}_{p6} = \begin{bmatrix} 0 & 0 & 0 & 0 & 0 & 0 \\ 0 & 0 & 0 & 0 & 0 & 0 \\ 0 & 0 & 0 & 0 & 0 & 0 \\ 0 & 0 & 0 & 0 & 0 & 0 \\ 0 & 0 & 0 & 0 & 0 & 0 \\ 0 & 0 & 0 & 0 & 0 & -g_6 \end{bmatrix} \tag{A.14}$$